THE UNIVERSITY OF MICHIGAN

COLLEGE OF ENGINEERING
DEPARTMENT OF ELECTRICAL ENGINEERING
SPACE PHYSICS RESEARCH LABORATORY

Annual Report No. 1

The Photoelectron Energy Distribution in the Ionosphere

Theoretical Study of the Moving Langmuir Probe in the Presence of a Magnetic Field

Theoretical Study of the Response of a Probe to Plasma Waves

UNPUBLISHED PRELIMINARY DATA

ERNEST G. FONTHEIM
WALTER R. HOEGY
MADHOO KANAL
ANDREW F. NAGY

GPO PRICE $ _____

OTS PRICE(S) $ _____

Hard copy (HC) 3.00

Microfiche (MF) .75

Under Contract With:

National Aeronautics And Space Administration
Grant No. NsG-525
Washington, D. C.

Administered through:

February 1965

THE UNIVERSITY OF MICHIGAN
COLLEGE OF ENGINEERING
Department of Electrical Engineering
Space Physics Research Laboratory

Annual Report No. 1

THE PHOTOELECTRON ENERGY DISTRIBUTION IN THE IONOSPHERE
THEORETICAL STUDY OF THE MOVING LANGMUIR PROBE IN THE PRESENCE OF A MAGNETIC FIELD
THEORETICAL STUDY OF THE RESPONSE OF A PROBE TO PLASMA WAVES

Ernest G. Fontheim
Walter R. Hoegy
Madhoo Kanal
Andrew F. Nagy

ORA Project 06106

under contract with:

NATIONAL AERONAUTICS AND SPACE ADMINISTRATION
GRANT NO. NsG-525
WASHINGTON, D.C.

administered through:

OFFICE OF RESEARCH ADMINISTRATION ANN ARBOR

February 1965

TABLE OF CONTENTS

LIST OF ILLUSTRATIONS

LIST OF ILLUSTRATIONS (Concluded)

I. INTRODUCTION

This report describes the work done under NASA Grant No. NsG-525 during the period 1 October 1963 to 30 September 1964. As the title of the grant indicates, the research effort was directed toward a better general understanding in the following areas:

A. the presence of plasma instabilities in the ionosphere and their effect on the thermal structure,

B. characteristics of probes in the ionosphere considering magnetic field effects and plasma waves.

Some of this work relating to Part A has been reported earlier,[1,2,3] and, therefore, that material will be outlined only briefly.

The initial work in the area of plasma instabilities consisted of the treatment of a one-dimensional Maxwellian plasma with a superposed high energy hump in the distribution function. High momentum transfer electron-neutral collisions were included in the treatment by means of a relaxation term in the kinetic equation. This work has shown that the temperature of certain plasmas, which are initially unstable against growing plasma waves, increases toward a temperature value for which the system is stable.[3]

In order to extend this work to ionospheric problems it became necessary to formulate a realistic model of the high energy tail of the electron energy distribution in the ionosphere. A preliminary calculation involving only one of the many possible photoionization processes has been presented

in the semiannual report.[3] The complete results involving all photoionization processes of importance are reported in Section II below.

The current collection equation of a stationary cylindrical probe in the presence of a magnetic field, parallel to its axis, was given in the semiannual report.[3] This work has been extended to the more general case of moving probes as given in Section III.

The results from the Alouette topside sounder satellite increased the interest for a better understanding of the excitation and detection mechanisms of space charge waves. Besides the fundamental interest in the possible existence of naturally occurring space charge waves, artificially excited waves could provide an excellent tool for the measurement of ambient electron densities. In such a technique a relatively large volume about the probe would be "sampled." therefore, if sufficiently good "coupling" can be achieved this approach might be especially valuable at high altitudes, where other direct techniques of sampling much smaller effective volumes become sensitivity limited. Theoretical work to predict the response of a cylindrical probe to such space charge waves has been started and is described in Section IV.

II. PHOTOELECTRON ENERGY DISTRIBUTION IN THE LOWER F-REGION

2.1 GENERAL CONSIDERATIONS

The state of the electrons in the ionosphere differs from an equilibrium state because of various energy and particle sources and sinks. The most significant as well as best known of these energy sources is the electromagnetic solar radiation. A considerable amount of this incoming energy first goes into the production of photoelectrons which, in turn, share their energy with neutrals, ambient electrons, and ions. Hanson,[4] and more recently, Dalgarno et al.[5] have calculated the steady-state electron temperature, considering a number of atmospheric conditions. In these calculations, solar electromagnetic radiation was considered to be the only heat source, and only binary collisions were included. These authors also assumed that all energy given up by the photons is deposited locally. Recently, Geisler and Bowhill[6] carried out detailed calculations using information from the work of Dalgarno et al.[5] in which they also included the effect of nonlocal heating, as well as conduction by ambient electrons. The calculations, however, do not consider long range electrostatic interactions (plasma oscillations). It has been suggested[1] that such an energy transfer mechanism may also be important because energy could then be transferred by relatively high energy photoelectrons to ambient electrons before they lose a considerable portion of their energy through binary collisions with neutrals and ions.

In order to study such an effect, we have proceeded in two steps. First the distribution of photoelectrons has been calculated assuming that the

photoelectrons interact with the ambient gas by binary collisions only. The resultant electron distribution is then assumed to be the sum of a Maxwellian distribution f_m at some temperature T_e plus the computed photoelectron energy distribution f. Considering this resultant distribution as an "initial" distribution the effects of long range interactions are included in the second step by using the self-consistent field method of Vlasov. Such a calculation will give a new electron distribution function modifying both the temperature of the ambient electron gas and the shape of the photoelectron distribution. So far, the calculations involving the first step have been completed and are reported in this section.

In the calculations it has been assumed that only photoelectrons contribute to the non-Maxwellian shape of the energy distribution. The effect of corpuscular radiation is not included since little reliable data are currently available. However, the calculations can be modified to include such an effect.

The assumption of the independence of the two component distribution functions should be elaborated. With f_m and f independent, f can be computed by fixing the ambient electron distribution f_m and calculating the energy loss of the energic photoelectrons as they traverse the ambient plasma. In other words, the energy loss is computed by considering the photoelectrons as test particles which are effected by the ambient particles but which themselves do not alter the ambient distribution. The assumption of independence fails, however, because the photoelectrons are continually interacting with the ambient electrons, ions, and neutrals. In fact, after a photoelectron

has suffered several collisions, it cannot be distinguished from an ambient electron—there is only one distribution function for all the electrons present. However, when the initial energy of the photoelectron is much higher than the average energy of the ambient electrons, it is possible to distinguish photoelectron from ambient electron. Then, to the extent that the photoelectron energy exceeds the average electron energy, the test particle assumption is valid and the two distributions f and f_m can be considered independent. A more exact solution would be found by solving the Boltzmann equation with a source term representing the production of photoelectrons and a sink term representing all processes which remove electrons. In this way, a steady-state electron distribution function would be obtained whose general appearance would be Maxwellian near the average kinetic energy with an increased high energy region similar to the curves in Fig. 2.5.

2.2 THE PHOTOELECTRON DISTRIBUTION FUNCTION

Let f(e) be the photoelectron energy distribution function, such that f(e)de gives the number of photoelectrons per unit volume in the energy interval e to e + de. Integrating this function over the interval E to ∞ gives the total number of photoelectrons per unit volume N(E) having energy greater than E, or

$$N(E) = \int_E^\infty f(e)de \ . \qquad (2.1)$$

Let q(E') be the photoelectron production rate, such that q(E')dE' is the rate at which photoelectrons are produced in the energy interval E' to

E' + dE', in units of number of electrons per sec per unit volume. Upon suffering collisions with ambients, the electrons lose energy and are spread into the interval E to E'(E<E') in a time T(E,E') given by,

$$T(E,E') = \int_{E}^{E'} \frac{de}{-r(e)} , \tag{2.2}$$

where r(E) = dE/dt is the energy loss rate. Thus the steady-state number of photoelectrons N(E,E'), residing in the energy interval E to E' due to production at energy E' is,

$$N(E,E') = T(E,E')q(E')dE' . \tag{2.3}$$

The total number of photoelectrons having energy greater than E is given by the integral of expression (2.3) over all production energies E' greater than E,

$$N(E) = \int_{E}^{\infty} N(E,E')dE' . \tag{2.4}$$

Equating expressions (2.1) and (2.4) and making use of (2.2) and (2.3) it is found that, after changing the order of integration,

$$\int_{E}^{\infty} f(e)de = \int_{E}^{\infty} \frac{de}{-r(e)} \int_{e}^{\infty} q(E')dE' . \tag{2.5}$$

Since the lower limit of integration E is arbitrary, the integrands must be equal, viz.

$$f(E) = \frac{Q(E)}{-r(E)} , \tag{2.6}$$

where $Q(E)$, the accumulated production rate, is defined by,

$$Q(E) \equiv \int_E^\infty q(E')dE' . \tag{2.7}$$

Thus the distribution function is the ratio of the accumulated production rate divided by the energy loss rate, and its properties can be discussed separately in terms of the two functions $r(E)$ and $Q(E)$.

The energy loss rate $r(E)$ is computed from binary collisions between energetic photoelectrons and ambient ions, electrons, and neutrals. The collision processes are many in number and the available cross section data are by no means complete. To avoid repetition of the calculations of Dalgarno *et al.*,[5] their energy loss computations are employed without change. The collision processes considered by Dalgarno are listed in Table I.

In Fig. 2.1 the spatial energy loss rates for electron-neutral and electron-electron collisions are plotted separately. The altitude dependence of the loss rates results from the altitude dependence of number density and composition. Considering first the r_N curves (electron-neutral collisions), the dominant contribution in the 5 eV to 15 eV range is from electronic excitation of O, O_2, and N_2. Below 5 eV this energy loss becomes insignificant. In the range from about 1.5 eV to 5 eV the predominant energy loss process is the vibrational excitation of N_2. Below 1.5 eV this process becomes negligible compared to the electron-electron loss, given by the r_e curves. The

TABLE I

TRANSITIONS TAKEN INTO ACCOUNT IN DERIVING THE ENERGY DISTRIBUTION OF PHOTOELECTRONS

Atomic Oxygen Transitions		
Electron removed	Resulting state of O^+	Threshold energy in eV
$2p$	^4S	13.6
$2p$	^2D	16.9
$2p$	^2P	18.7
$2s$	^4P	28.5
$2s$	^2P	40.0

Molecular Oxygen Transitions		
Electron removed	Resulting state of O_2^+	Threshold energy in eV
$\pi_g 2p$	$^2\pi_g$	12.1
$\pi_u 2p$	$^4\pi_u$	16.2
$\pi_u 2p$	$^2\pi_u$	17.0
$\sigma_g 2p$	$^4\Sigma_g^-$	18.2
$\sigma_u 2s$	$^2\pi_u$	~ 28
$\sigma_g 2s$	$^2\pi_g$	~ 40

Molecular nitrogen transitions		
Electron removed	Resulting state of N_2^+	Threshold energy in eV
$\sigma_g 2p$	$^2\Sigma_g^+$	15.6
$\pi_u 2p$	$^2\pi_u$	16.7
$\sigma_u 2s$	$^2\Sigma_u^+$	18.8
$\sigma_g 2s$	$^2\Sigma_g^+$	~ 35

r_e loss curves were computed analytically by Butler and Buckingham.[7]

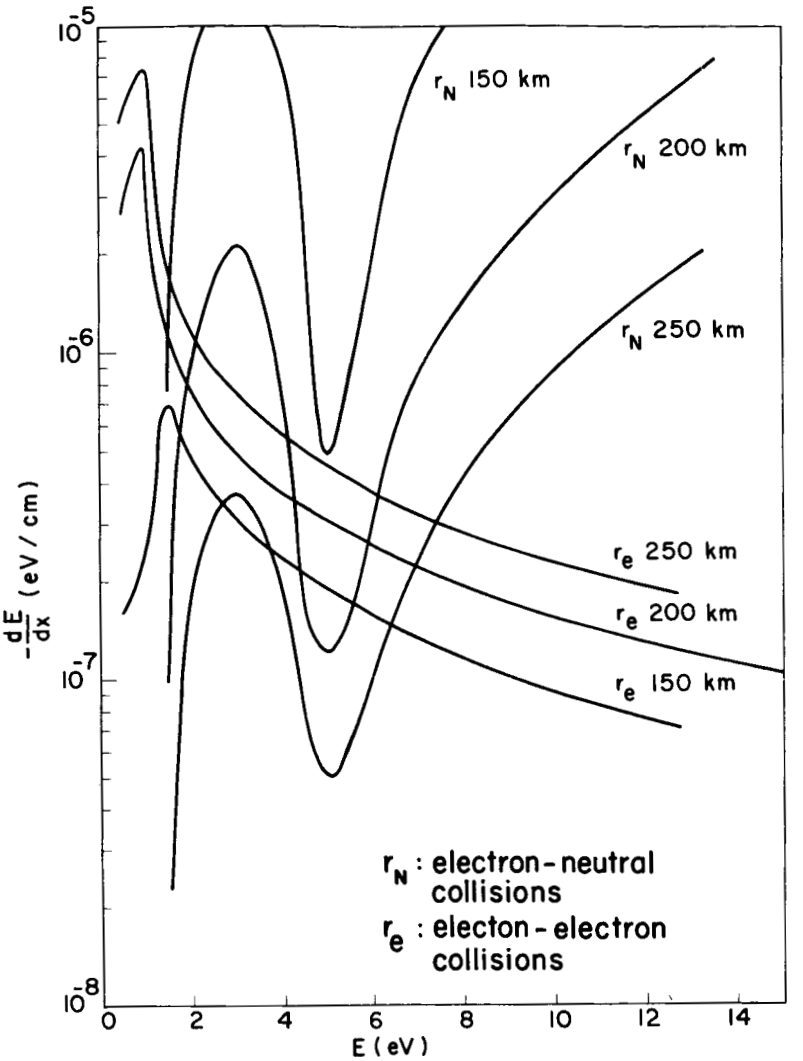

Fig. 2.1. Energy loss rates vs. energy.

In Fig. 2.2 the total time rates of energy loss are given for the three altitudes 150, 200, and 250 km. The minimum at around 5 eV is connected with the rapid decrease in both the vibrational excitation of N_2 and the electronic excitation of O, O_2, and N_2. The maximum at around 3 eV is connected with the high rate of energy loss in vibrational excitation of N_2. The increase in loss rate below 1.5 eV is connected with the high probability of electron-electron collisions. It is to be noted that the general behavior of the energy dis-

tribution curve will follow closely the inverse of the loss curve.

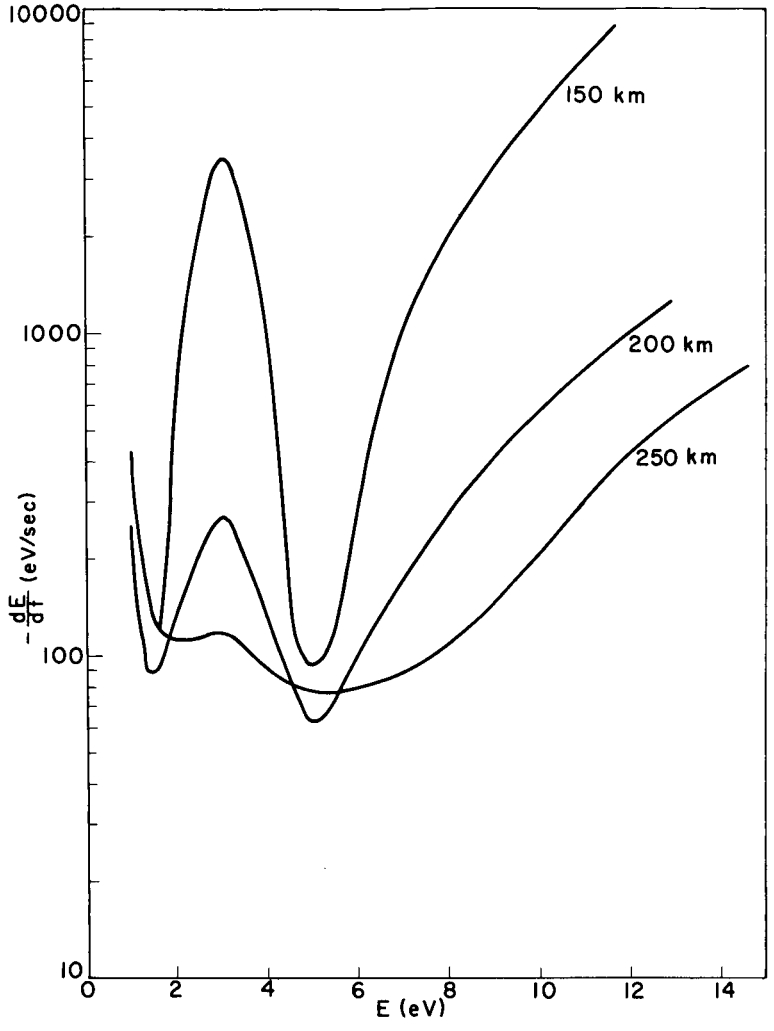

Fig. 2.2. Total energy loss rates vs. energy.

The accumulated production rate Q(E), found by adding all the contributions to the production rate q at energies greater than E, is computed from the most recent data on photon flux[8] and photoionization cross sections.[8] The photoelectron production rate is the product of neutral particle density, photoionization cross section, and photon flux. Photoionization of O, O_2, and N_2 is included.

The result of these computations is given in Fig. 2.3. The altitude dependence of the accumulated production rate follows the altitude variation

of neutral particle density and solar transmission coefficients. Since the photoelectron distribution function is directly proportional to the accumulated production rate Q, it is observed from Fig. 2.3 that the Q curves only slightly modify the distribution until an energy of about 15 eV where they rapidly cut off the distribution function.

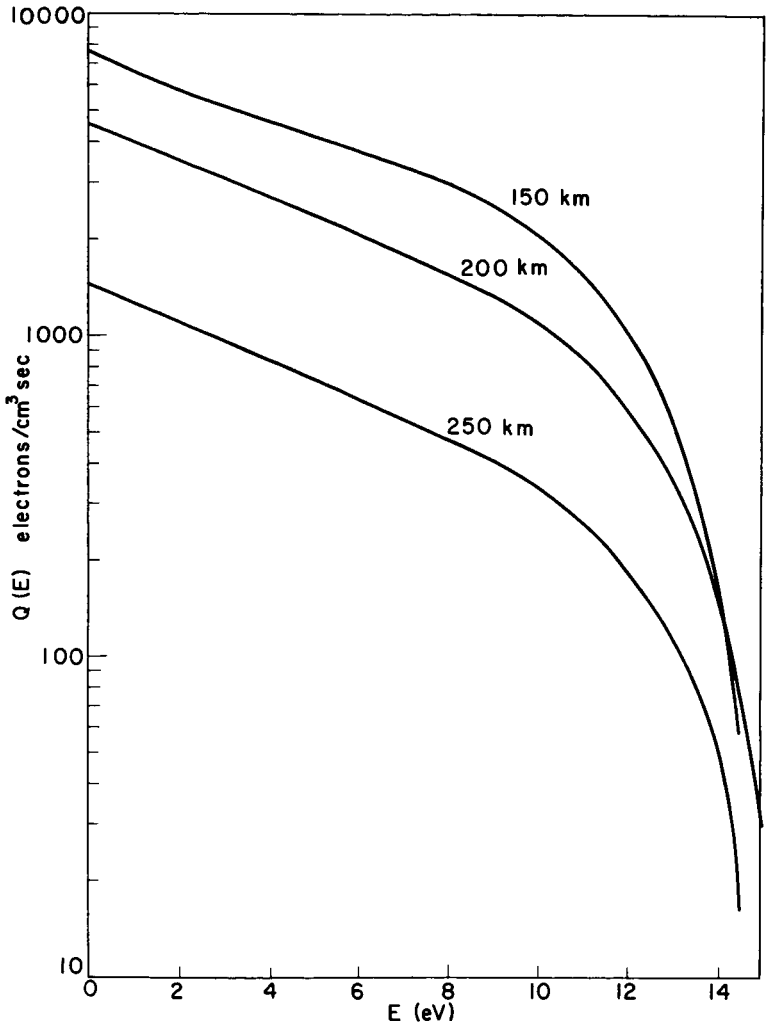

Fig. 2.3. Accumulated production rate vs. energy.

The energy distribution function f, product of the Q curves and the 1/r curves, is presented in Fig. 2.4. For energies above 10 eV the number of photoelectrons decreases very rapidly due to the cut-off behavior of the Q curves. A hump or maximum occurs at around 5 eV as a result of the simultaneous

decrease in vibrational and electronic excitation energy losses which "trap" the photoelectrons in this region. The trough at around 3 eV is connected with the peak in energy loss to vibrational excitation of N_2. As a result of this peak, fewer electrons are allowed to remain at this energy. The distribution function increases below 3 eV to a second hump at around 1.5 eV corresponding to the decrease in vibrational energy loss. Below this energy the dominant electron-electron energy loss increases, causing a rapid decrease in the number of photoelectrons toward lower energy values.

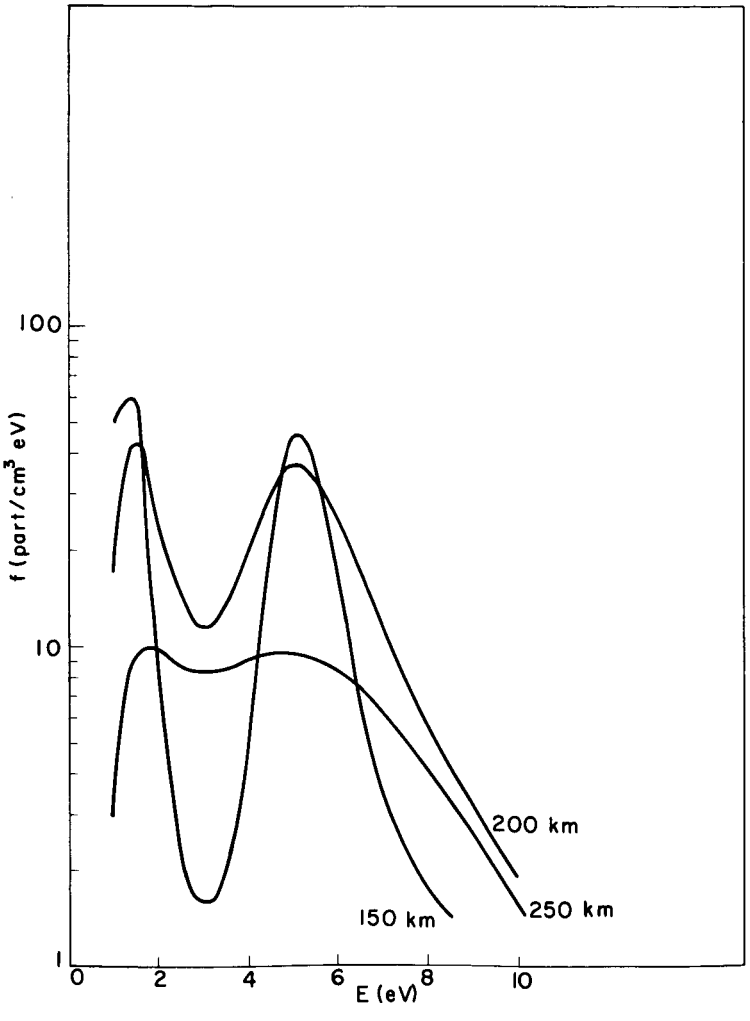

Fig. 2.4. Photoelectron energy distribution f(E) vs. energy E at the three altitudes 150, 200, and 250 km.

The total electron energy distribution function is the sum of the above photoelectron energy distribution function and an appropriately chosen Maxwellian distribution. Fig. 2.5 illustrates the total energy distribution for

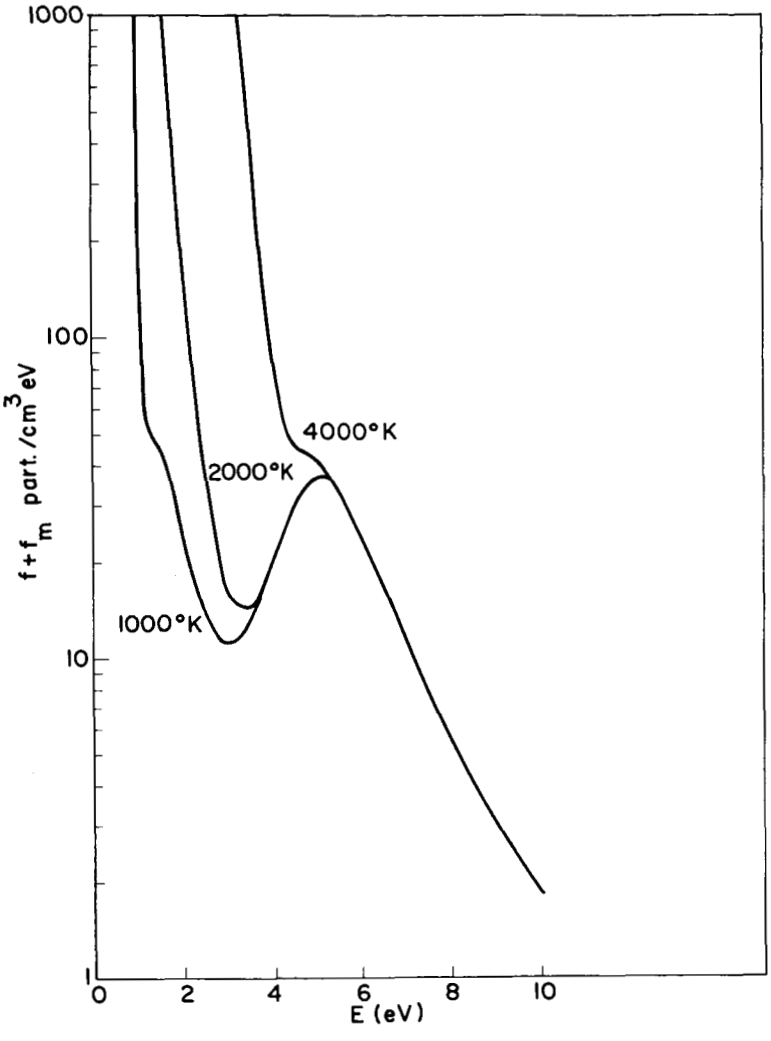

Fig. 2.5. Total energy distribution $f + f_m$ vs. energy at 200 km for electron temperatures of 1000°K, 2000°K, and 4000°K.

the three temperatures, 1000, 2000, and 4000°K at an altitude of 200 km. The character of the high-energy hump is highly dependent on the ambient electron temperature chosen. At the two lower temperatures the hump is clearly evident. At some temperature just below 4000°K, the hump disappears, and for all higher temperatures there is no hump at all, but merely a raised high energy tail.

The daytime temperature at an altitude of 200 km is about 2500°K. Hence, we conclude that in the absence of long-range interactions the electron energy distribution displays a hump on its high energy tail.

III. THEORY OF CURRENT COLLECTION BY MOVING CYLINDRICAL PROBES IN THE PRESENCE OF A MAGNETIC FIELD

3.1 EQUATIONS OF MOTION

The work leading to the equations of current collection by a moving cylindrical probe in the presence of an axial magnetic field is outlined in this section. In the general case a uniform magnetic field of intensity $\vec{B}$ is oriented in a direction which makes an arbitrary angle α with the axis of the cylindrical collector, as shown in Fig. 3.1. Let a denote the radius of the

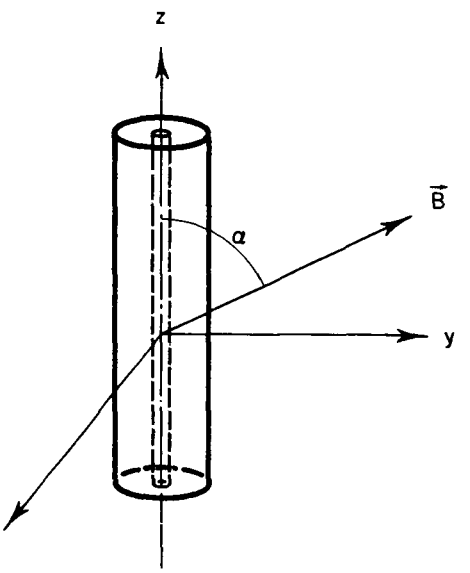

Fig. 3.1. Cylindrical probe in a magnetic field.

sheath, r_c the radius of the collector, ℓ its length ($\ell \gg r_c$), and Φ the potential at any point in the sheath with respect to the neutral plasma. If Φ is a function of r only, with $r^2 = x^2 + y^2$, then the electric field intensity $E = -d\Phi/dr$.

The force $\vec{F}$ experienced by a charged particle of mass m and charge q moving with velocity $\vec{u}$ in the sheath in the presence of an electric field $\vec{E}$ and a magnetic field $\vec{B}$ is given by the Lorentz equation:

$$\vec{F} = q[\vec{E}+\vec{u}\times\vec{B}] \ . \tag{3.1}$$

The components of the acceleration along the x, y, and z axes, respectively, are

$$\begin{aligned} \ddot{x} &= \frac{q}{m}\,[E_x-\dot{y}B_z+\dot{z}B_y] \ , \\ \ddot{y} &= \frac{q}{m}\,[E_y-\dot{z}B_x+\dot{x}B_z] \ , \\ \ddot{z} &= \frac{q}{m}\,[\dot{y}B_x-\dot{x}B_y] \ , \end{aligned} \tag{3.2}$$

where dots represent the time derivatives and B_x, B_y, B_z are the components of $\vec{B}$ along the corresponding axes.

The system of equations given in (3.2) can be easily solved if $B_x = B_y = 0$. In that case let $B_z = B$ and reduce the system to:

$$\begin{aligned} \ddot{x} &= \frac{q}{m}\,[E_x-\dot{y}B] \ , \\ \ddot{y} &= \frac{q}{m}\,[E_y+\dot{x}B] \ , \\ \ddot{z} &= 0 \ . \end{aligned} \tag{3.3}$$

To obtain the relation between the angular momenta of a particle at the sheath edge and inside the sheath, multiply the first equation in (3.3) by

y, the second equation by x and subtract. Note the fact that $yE_x - xE_y = 0$, since $\vec{E}$ is a radial field. Thus,

$$\frac{d}{dt}(y\dot{x}-x\dot{y}) = -\frac{\omega}{2}\frac{d}{dt}(x^2+y^2) .$$

This gives us,

$$y\dot{x} - x\dot{y} = -\frac{\omega}{2}(x^2+y^2) + c_1 , \qquad (3.4)$$

where $\omega = qB/m$ is the cyclotron frequency, and c_1 is the constant of integration to be determined by the initial values of the position and the velocity of the particle at the sheath edge. If we transform Eq. (3.4) from the cartesian rectangular coordinate system to polar coordinates by putting $x = r\cos\theta$, $y = r\sin\theta$ we obtain

$$-r^2\left(\frac{d\theta}{dt}\right) = -\frac{\omega}{2}r^2 + c_1 .$$

Then employing the initial values, i.e., at $r = a$, $a\, d\theta/dt = u_t$, where u_t is the tangential velocity component of the particle at the sheath edge, we get

$$r^2\frac{d\theta}{dt} = ru_t' = -\frac{\omega}{2}(a^2-r^2) + au_t , \qquad (3.5)$$

where u_t' is the tangential velocity component of the particle inside the sheath.

The corresponding relation between the energy of the particle at the sheath edge and that inside the sheath may be obtained from (3.3) by multiplying the first equation by $\dot{x}$ and the second equation by $\dot{y}$. Then on adding the

two equations, we get

$$\dot{x}\ddot{x} + \dot{y}\ddot{y} = \frac{q}{m} [\dot{x}E_x + \dot{y}E_y] \quad .$$

In polar coordinates this becomes

$$\frac{d}{dt} (u_r'^2 + u_t'^2) = \frac{2q}{m} E \frac{dr}{dt} = - \frac{d\Phi}{dt} \quad ,$$

where $-u_r' = dr/dt$ is the radial velocity of the particle inside the sheath. u_r' has been defined in such a way that it is positive for a particle traveling toward the probe. Integration of the above equation with respect to t yields

$$u_r'^2 + u_t'^2 = - \frac{2q}{m} \Phi + c_2 \quad ,$$

where c_2 is the constant of integration to be determined from the initial values. If at $r = a$, $\Phi = 0$, $u_r' = u_r$, and $u_t' = u_t$, then we get,

$$u_r'^2 + u_t'^2 = - \frac{2q}{m} \Phi + u_r^2 + u_t^2 \quad . \tag{3.6}$$

In order to obtain the condition of collection we require that u_r' be real and positive at the collector surface. Hence, at the collector surface Eqs. (3.5) and (3.6) become, after setting $u_r'^2 \geq 0$,

$$u_{tc}' = - \frac{\omega}{2} \frac{a^2 - r_c^2}{r_c} + \frac{a}{r_c} u_t \tag{3.7}$$

$$u_{tc}'^2 \leq u_r^2 + u_t^2 - \frac{2qV}{m} \quad , \tag{3.8}$$

where u'_{tc} is the tangential velocity component at the collector surface and $V = \Phi(r_c)$ is the probe potential, i.e., the voltage of the collector with respect to the plasma. Elimination of u'_{tc} between (3.7) and (3.8) yields

$$\left(\frac{a}{r_c} u_t - \frac{\omega}{2} \frac{a^2 - r_c^2}{r_c} \right)^2 \leq u_r^2 + u_t^2 - \frac{2qV}{m}$$

or

$$\frac{\omega a}{2} - \sqrt{\frac{r_c^2}{a^2 - r_c^2} \left(u_r^2 - \frac{2qV}{m} \right) + \frac{\omega^2 r_c^2}{4}} \leq u_t$$

$$\leq \frac{\omega a}{2} + \sqrt{\frac{r_c^2}{a^2 - r_c^2} \left(u_r^2 - \frac{2qV}{m} \right) + \frac{\omega^2 r_c^2}{4}} \quad . \tag{3.9}$$

Equation (3.9) defines the range of u_t for which a particle with a given u_r is collected. Graphically this range can be represented by the area bounded by the two branches of the hyperbola

$$u_t = \frac{\omega a}{2} \pm \sqrt{\frac{r_c^2}{a^2 - r_c^2} \left(u_r^2 - \frac{2qV}{m} \right) + \frac{\omega r_c^2}{4}} \quad , \qquad (u_r > 0)$$

as shown by Figs. 3.2(a) and 3.2(b) for the case $qV < 0$, i.e., for a particle which is accelerated by the collector potential. The vertices p_1 and p_2 of the hyperbola are

$$p_1 = \frac{\omega a}{2} - \sqrt{\frac{\omega^2 r_c^2}{4} - \frac{r_c^2}{a^2 - r_c^2} \frac{2qV}{m}}$$

$$p_2 = \frac{\omega a}{2} + \sqrt{\frac{\omega^2 r_c^2}{4} - \frac{r_c^2}{a^2 - r_c^2} \frac{2qV}{m}} \quad . \tag{3.10}$$

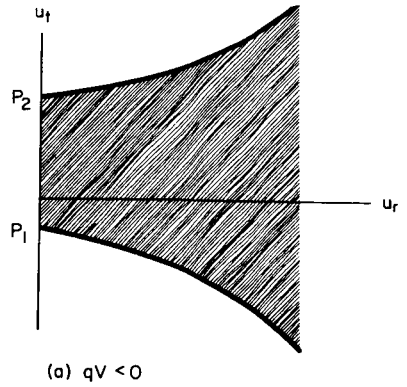

(a) $qV < 0$

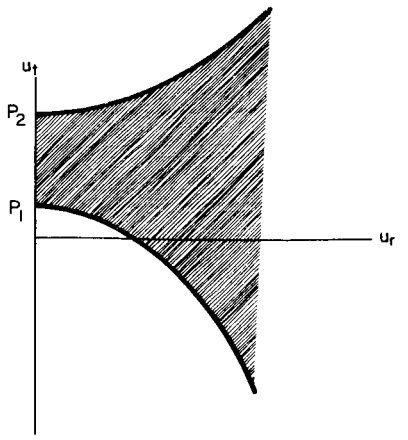

(b) $qV \lesseqgtr 0$

(a) $qV<0$ (accelerating potential) with

$$\frac{\omega a}{2} < \sqrt{\frac{\omega^2 r_c^2}{4} - \frac{r_c^2}{a^2-r_c^2}\frac{2qV}{m}}$$

(b) $qV<0$ (accelerating potential) with

$$\frac{\omega a}{2} > \sqrt{\frac{\omega^2 r_c^2}{4} - \frac{r_c^2}{a^2-r_c^2}\frac{2qV}{m}}$$

and

$qV > 0$ (retarding potential) with

$$qV \leq \frac{\omega^2(a^2-r_c^2)m}{8} \quad , \qquad u_r^2 \geq 0$$

Fig. 3.2 Domain of integration for the current Eq. (3.19) for the above cases.

If

$$\frac{\omega a}{2} < \sqrt{\frac{\omega^2 r_c^2}{4} - \frac{r_c^2}{a^2-r_c^2}\frac{2qV}{m}} \quad , \tag{3.11a}$$

the area is shown by Fig. 3.2(a), while for

$$\frac{\omega a}{2} > \sqrt{\frac{\omega^2 r_c^2}{4} - \frac{r_c^2}{a^2-r_c^2}\frac{2qV}{m}} \tag{3.11b}$$

the area is shown by Fig. 3.2(b). If $qV > 0$, i.e., if the particle is retarded by the collector potential, either of the following two conditions must be

satisfied in order for the expression under the square root in Eq. (2.9) to be non-negative,

$$qV \leq \frac{\omega^2(a^2-r_c^2)m}{8} \quad , \qquad u_r^2 \geq 0 \tag{3.12a}$$

$$qV \geq \frac{\omega^2(a^2-r_c^2)m}{8} \quad , \qquad u_r^2 \geq \frac{2qV}{m} - \frac{\omega^2(a^2-r_c^2)}{4} \quad . \tag{3.12b}$$

In the case of condition (3.12a) the range of allowed values is again represented by the shaded area between the two hyperbolas shown in Fig. 3.2(b). Since

$$\sqrt{-\frac{r_c^2}{a^2-r_c^2}\frac{2qV}{m} + \frac{\omega^2 r_c^2}{4}} \leq \frac{\omega r_c}{2} \leq \frac{\omega a}{2},$$

it follows that $p_1 \geq 0$ always. If, on the other hand, the probe potential satisfies the inequality (3.12b), then the range of values of (u_r,u_t), for which a particle will be collected, is given by the area bounded by the conjugate hyperbola shown in Fig. 3.3. Thus, under the conditions specified

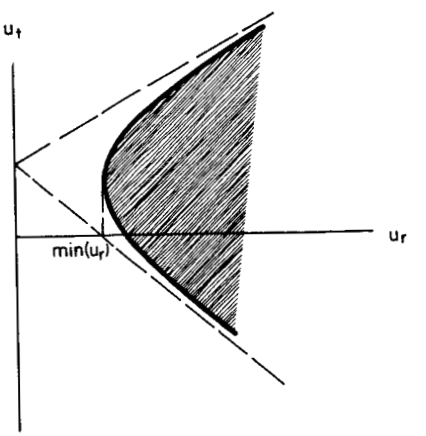

Fig. 3.3. Domain of integration for the current Eq. (3.19) for the case $qV > 0$ (retarding potential) with

$$qV \geq \frac{\omega^2(a^2-r^2)m}{8} \quad , \qquad u_r^2 \geq \frac{2qV}{m} - \frac{\omega^2(a^2-r^2)}{4}$$

above, Figs. 3.2(a), 3.2(b), and 3.3 show the domains of permissible velocities of the particles at the sheath edge which will reach the collector and contribute to the total current to the probe.

At this stage it is desirable to change the variables in Eqs. (3.7) and (3.8) by setting $u_r = u\cos\theta$, $u_t = u\sin\theta$. Here θ is the angle which the particle velocity at the sheath edge makes with the radius vector. This is done because, for the case of the moving probe, the subsequent integrations to obtain the corresponding current equations for $qV > 0$ and $qV < 0$ are considerably simplified when the variables of integration are u and θ. Thus in terms of u and θ the range defined by relation (3.9) is given by

$$\sin^{-1}\left[\frac{\omega}{2u}\,\frac{a^2-r_c^2}{a} - \frac{r_c}{au}\sqrt{u^2 - \frac{2qV}{m}}\right] \leq \theta$$

$$\leq \sin^{-1}\left[\frac{\omega}{2u}\,\frac{a^2-r_c^2}{a} + \frac{r_c}{au}\sqrt{u^2 - \frac{2qV}{m}}\right], \qquad (3.13)$$

where for uniqueness θ has to be chosen such that

$$-\frac{\pi}{2} \leq \theta \leq \frac{\pi}{2} \quad .$$

Now we will set up a general expression in the integral form which will represent the current of either sign to the probe and then integrate it over the domains for $qV < 0$ and $qV > 0$ (as given above) to obtain the corresponding current equations.

3.2 GENERAL EXPRESSION FOR THE CURRENT

The plasma is assumed to have a Maxwellian velocity distribution at the sheath edge. If the probe is stationary, this distribution is given by

$$F(u_{r_o},u_{t_o},u_{z_o}) = \frac{N}{\pi^{3/2}c^3} \exp\left[-\frac{1}{c^2}(u_{r_o}^2+u_{t_o}^2+u_{z_o}^2)\right] , \qquad (3.14)$$

where N is the number density of the particles under consideration and c is their most probable velocity, i.e., $c = \sqrt{2kT/m}$; where k is Boltzmann's constant, T is the temperature of the medium, and m is the mass of the particle. u_{r_o}, u_{t_o}, and u_{z_o} are the components of the particle velocity in a frame of reference fixed in space. When the probe is moving, let u_r, u_t, and u_z denote the components of the particle velocity in a probe-fixed coordinate system with z-axis along the probe axis. Then,

$$\begin{aligned} u_{r_o} &= u_r - W \sin\phi \cos\beta \\ u_{t_o} &= u_t - W \sin\phi \sin\beta \\ u_{z_o} &= u_z - W \cos\phi , \end{aligned}$$

where $\vec{W}$ is the probe velocity, ϕ is the angle between $\vec{W}$ and the axis of the cylinder, and β is the angle between the projection of $\vec{W}$ on the plane perpendicular to the z-axis and the radius vector $\vec{r}$. In terms of the new coordinates (3.14) becomes

$$f(u_r,u_t,u_z) = \frac{N}{\pi^{3/2}c^3} \exp\left[-\frac{1}{c^2}\{(u_r-W\sin\phi\cos\beta)^2 + (u_t-W\sin\phi\sin\beta)^2 + (u_z-W\cos\phi)^2\}\right] . \qquad (3.15)$$

The number of particles crossing an infinitesimal strip of area $\ell a d\beta$ of the sheath surface per unit time is

$$u_r dN = \ell a u_r f(u_r,u_t,u_z)\, du_r du_t du_z d\beta , \qquad (3.16)$$

where ℓ is the length of the cylinder. On multiplying this expression with

the charge q of the particle and integrating over the desired limits, the following equation for the current to the probe is obtained:

$$I = \frac{Nq\ell a}{\pi^{3/2}c^3}\int_{\beta}\int_{u_r}\int_{u_t}\int_{u_z} u_r \exp\left[-\frac{1}{c^2}\{(u_r - W\sin\phi\cos\beta)^2 + (u_t - W\sin\phi\sin\beta)^2 + (u_z - W\cos\phi)^2\}\right] du_r du_t du_z d\beta \ . \qquad (3.17)$$

In both cases of current collection ($qV < 0$ and $qV > 0$) the limits of β and u_z are $0 \le \beta \le 2\pi$ and $-\infty < u_z < \infty$ (since $\ell \gg a$), respectively. The integration of (3.17) with respect to these two variables and rearrangement of the terms yields,

$$I = 2Nq\ell a c^{-2} e^{-\kappa^2}\int_{u_r}\int_{u_t} u_r \exp\left[-\frac{1}{c^2}(u_r^2+u_t^2)\right] I_o\left(\frac{2\kappa}{c}\sqrt{u_r^2+u_t^2}\right) du_r du_t \ , \qquad (3.18)$$

where $\kappa = (W\sin\phi)/c$ and $I_o(x)$ is the modified Bessel function of order zero. Integration of (3.18) is greatly simplified by setting $u_r = u\cos\theta$, $u_t = u\sin\theta$. Thus

$$I = \frac{2}{\sqrt{\pi}}\frac{a}{r_c}\frac{J}{c^3} e^{-\kappa^2}\int_{u}\int_{\theta} u^2\cos\theta\, e^{-u^2/c^2} I_o\left(2\kappa\frac{u}{c}\right) du\, d\theta \ , \qquad (3.19)$$

where $J = \sqrt{kT/2m\pi}\, Nq2\pi\ell r_c$ is the random current to the probe. Equation (3.19) is the general expression for the current collected by a moving cylindrical probe of length ℓ and radius r_c surrounded by a sheath of radius a. The area of integration is determined by the different cases of interest (i.e., accelerated current, retarded current, etc.), as discussed in the preceding section.

3.3 ACCELERATED CURRENT ($qV < 0$)

We have already seen that when the particles are accelerated by the collector potential, the domain of integration is given by Eq. (3.13) with $qV < 0$ and is represented graphically by Figs. 3.2(a) and 3.2(b) in association with the inequalities (3.11a) and (3.11b), respectively. Let us, first, consider the situation where the inequality (3.11a) holds, i.e.,

$$\frac{\omega a}{2} < \sqrt{\frac{\omega^2 r_c^2}{4} - \frac{r_c^2}{a^2 - r_c^2}\frac{2qV}{m}} \quad . \tag{3.11a}$$

Upon dividing both sides of (3.11a) by $c = \sqrt{2kT/m}$ and letting $\omega/2c = \sigma$, $2qV/mc^2 = qV/kT = V_o$ and $\tau^2 = r_c^2/(a^2 - r_c^2)$, relation (3.11a) becomes

$$\sigma a < \sqrt{\sigma r_c^2 - \tau^2 V_o} \quad . \tag{3.20}$$

In order to integrate (3.19), the shaded region in Fig. 3.2(a) is divided into three regions R_1, R_2, and R_3 as shown in Fig. 3.4(a).

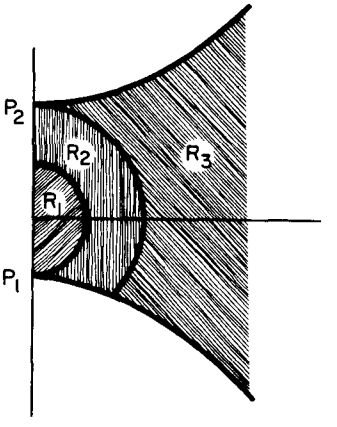

Fig. 3.4(a). Domain of integration for the case shown in Fig. 3.2(a) indicating the three subregions into which the domain has been decomposed for purposes of integration.

Let us consider the integral

$$\mathcal{I} = \iint_R G \cos\theta \, du \, d\theta \, ,$$

where $G = u^2 e^{-u^2/c^2} I_o\left(2 \frac{u}{c} \kappa\right)$ and $R = R_1 \cup R_2 \cup R_3$. Thus

$$\mathcal{I} = \iint_R = \iint_{R_1} + \iint_{R_2} + \iint_{R_3}$$

$$= \int_o^{|P_1|} \int_{-\pi/2}^{\pi/2} G \cos\theta \, du \, d\theta + \int_{|P_1|}^{P_2} \int_{\theta=\theta_1}^{\pi/2} G \cos\theta \, du \, d\theta + \int_{P_2}^{\infty} \int_{\theta_1}^{\theta_2} G \cos\theta \, du \, d\theta$$

where

$$\theta_1 = \sin^{-1}\left[\frac{\omega}{2u}\left(\frac{a^2 - r_c^2}{a}\right) - \frac{r_c}{au}\sqrt{u^2 - \frac{2qV}{m}}\right] \quad \text{and}$$

$$\theta_2 = \sin^{-1}\left[\frac{\omega}{2u}\left(\frac{a^2 - r_c^2}{a}\right) + \frac{r_c}{au}\sqrt{u^2 - \frac{2qV}{m}}\right]$$

and p_1 and p_2 are given by (3.10). After integrating with respect to θ we get,

$$\mathcal{I} = 2\int_o^{|P_1|} G \, du + \int_{|p_1|}^{P_2} G(1 - \sin\theta_1) du + \int_{p_2}^{\infty} G(\sin\theta_2 - \sin\theta_1) du$$

$$= \int_o^{|P_1|} G \, du + \int_o^{P_2} G \, du - \int_{|P_1|}^{P_2} G \sin\theta_1 du + \int_{p_2}^{\infty} G(\sin\theta_2 - \sin\theta_1) du \quad .$$

Taking each integral separately and integrating one obtains

$$A = \int_0^{|p_1|} G\, du = \int_0^{|p_1|} du\, u^2 e^{-u^2/c^2} I_0\left(2\kappa \frac{u}{c}\right)$$

$$= c^3 \sum_{n=0}^{\infty} \frac{\kappa^{2n}}{(n!)^2} \int_0^{|p_1|} \left(\frac{u}{c}\right)^{2n+2} e^{-u^2/c^2} \frac{du}{c}$$

$$= \frac{c^3}{2} \sum_{n=0}^{\infty} \frac{\kappa^{2n}}{(n!)^2} \int_0^{p_1^2/c^2} x^{n+1/2} e^{-x} dx \quad , \quad \text{where}$$

$$\frac{u^2}{c^2} = x \quad , \quad u\, du = \frac{c^2}{2} dx \quad .$$

$$= \frac{c^3}{2} \sum_{n=0}^{\infty} \frac{\kappa^{2n}}{(n!)^2} \gamma\left(n + \frac{3}{2}, \frac{p_1^2}{c^2}\right) \quad ,$$

where $\gamma(\alpha,x) = \int_0^x e^{-t} t^{\alpha-1} dt$ is the incomplete Gamma function. Similarily,

$$B = \int_0^{p_2} G\, du$$

$$= \frac{c^3}{2} \sum_{n=0}^{\infty} \frac{\kappa^{2n}}{(n!)^2} \gamma\left(n + \frac{3}{2}, \frac{p_2^2}{c^2}\right)$$

$$C = \int_{|p_1|}^{p_2} G \sin\theta_1\, du$$

$$= \int_{|p_1|}^{p_2} u^2 e^{-u^2/c^2} I_0\left(2\kappa \frac{u}{c}\right) \left\{\frac{\omega}{2u}\left(\frac{a^2 - r_c^2}{a}\right) - \frac{r_c}{au}\sqrt{u^2 - \frac{2qV}{m}}\right\} du$$

$$= \frac{\omega}{2}\left(\frac{a^2-r_c^2}{a}\right)\int_{|p_1|}^{p_2} u\, e^{-u^2/c^2} I_o\left(2\kappa \frac{u}{c}\right) du - \frac{r_c}{a}\int_{|p_1|}^{p_2} u\, e^{-u^2/c^2} I_o\left(2\kappa \frac{u}{c}\right)\sqrt{u^2 - \frac{2qV}{m}}\, du \,.$$

Also

$$D = \int_{p_2}^{\infty} G(\sin\theta_2 - \sin\theta_1) = 2\,\frac{r_c}{a}\int_{p_2}^{\infty} u\, e^{-u^2/c^2} I_o\left(2\kappa \frac{u}{c}\right)\sqrt{u^2 - \frac{2qV}{m}}\, du \,.$$

$$\therefore -C+D = -\frac{\omega}{2}\left(\frac{a^2-r_c^2}{a}\right)\int_{|p_1|}^{p_2} u\, e^{-u^2/c^2} I_o\left(2\kappa \frac{u}{c}\right)$$

$$+ \frac{r_c}{a}\left[\int_{|p_1|}^{\infty} + \int_{p_2}^{\infty}\right] u\, e^{-u^2/c^2} I_o\left(2\kappa \frac{u}{c}\right)\sqrt{u^2 - \frac{2qV}{m}}\, du \,.$$

Here

$$\int_{|p_1|}^{p_2} u\, e^{-u^2/c^2} I_o\left(2\kappa \frac{u}{c}\right) du = \frac{c^2}{2}\sum_{n=o}^{\infty} \frac{\kappa^{2n}}{(n!)^2}\left[\gamma\left(n+1, \frac{p_2^2}{c^2}\right) - \gamma\left(n+1, \frac{p_1^2}{c^2}\right)\right]$$

and

$$\left[\int_{|p_1|}^{\infty} + \int_{p_2}^{\infty}\right] u\, e^{-u^2/c^2} I_o\left(2\kappa \frac{u}{c}\right)\sqrt{u^2 - \frac{2qV}{m}}\, du$$

$$= \frac{c^3}{2}\, e^{-V_o} \sum_{n=o}^{\infty} \frac{\kappa^n}{n!(-V_o)^{n/2}} J_n(2\kappa\sqrt{-V_o})\left[\Gamma\left(n+\frac{3}{2}, \frac{p_1^2}{c^2} - V_o\right) + \Gamma\left(n+\frac{3}{2}, \frac{p_2^2}{c^2} - V_o\right)\right] ,$$

where

$$\Gamma(\nu,x) = \int_x^\infty e^{-t} t^{\nu-1} dt \ .$$

This last integration has been carried out in detail in an earlier paper.[10]

Substitution of the results A, B, -C+D, into Eq. (3.14) yields the expression for the accelerated current for the case $\sigma a < \sqrt{\sigma^2 r_c^2 - \tau^2 V_o}$,

$$I_{a_1} = \frac{J_a}{\sqrt{\pi}} e^{-\kappa^2} \left[\frac{a}{r_c} \sum_{n=0}^{\infty} \frac{\kappa^{2n}}{(n!)^2} \left\{ \gamma\left(n + \frac{3}{2}, \frac{p_1^2}{c^2}\right) + \gamma\left(n + \frac{3}{2}, \frac{p_2^2}{c^2}\right) - \frac{\sigma r_c^2}{\tau^2 a} \left(\gamma\left(n+1, \frac{p_2^2}{c^2}\right) \right.\right.\right.$$

$$\left.\left.\left. - \gamma\left(n+1, \frac{p_1^2}{c^2}\right) \right) \right\} + e^{-V_o} \sum_{n=0}^{\infty} \frac{\kappa^n}{n!(-V_o)^{n/2}} \left\{ \Gamma\left(n + \frac{3}{2}, \frac{p_1^2}{c^2} - V_o\right) \right.\right.$$

$$\left.\left. + \Gamma\left(n + \frac{3}{2}, \frac{p_2^2}{c^2} - V_o\right) \right\} J_n(2\kappa\sqrt{-V_o}) \right] , \qquad (3.21)$$

where

$$\frac{p_1}{c} = \sigma a - \sqrt{\sigma^2 r_c^2 - \tau^2 V_o} \quad , \qquad \frac{p_2}{c} = \sigma a + \sqrt{\sigma^2 r_c^2 - \tau^2 V_o}$$

and $J_a = \sqrt{kT/2m\pi} \cdot N q_a 2\pi \ell r_c$ is the random current to the probe of the accelerated particles of charge q_a.

Equation (3.21) reduces to the following form when $\kappa = 0$, which occurs either when the probe is stationary ($w = 0$) or when $\theta = 0°$

$$I_a\Big|_{\kappa=0} = \frac{J_a}{2} \left[\frac{a}{r_c} \{ \mathrm{erf}(\sqrt{\sigma^2 r_c^2 - \tau^2 V_o} - \sigma a) + \mathrm{erf}(\sqrt{\sigma^2 r_c^2 - \tau^2 V_o} + \sigma a) \} \right.$$

$$+ e^{-V_o} \{ \mathrm{erfc}(\sqrt{\sigma^2 a^2 - (1+\tau^2) V_o} - \sigma r_c)$$

$$\left. + \mathrm{erfc}(\sqrt{\sigma^2 a^2 - (1+\tau^2) V_o} + \sigma r_c) \} \right] , \qquad (3.22)$$

where $p_1/c = \sigma a - \sqrt{\sigma^2 r_c^2 - \tau^2 V_o}$ has been replaced by $-p_1/c$ since the limit of integration is $|p_1|$, and $p_1/c < 0$. Equation (3.22) has been reported earlier.[3]

Several other cases of interest which arise by setting $\sigma = 0$ (i.e., $B = 0$) in Eqs. (3.21) and (3.22) have been discussed in full detail earlier.[10]

When the inequality (3.11b) holds, i.e., if

$$\sigma a > \sqrt{\sigma^2 r_c^2 - \tau^2 V_o} \quad , \tag{3.23}$$

then the domain of integration of (3.19) is represented graphically by Fig. 3.2(b). As before, the region is divided into two regions R_1 and R_2 as shown in Fig. 3.4(b).

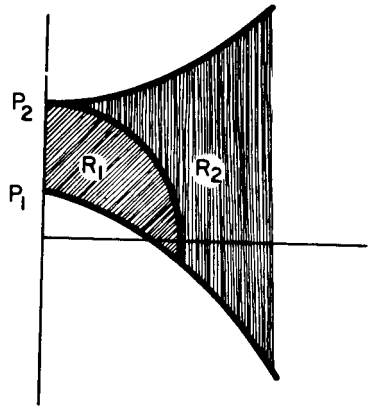

Fig. 3.4(b). Domain of integration for the cases shown in Fig. 3.2(b) indicating the two subregions into which the domain has been decomposed for purposes of integration.

Thus,

$$\mathcal{I} = \iint_{R_1} G\cos\theta\, du\, d\theta + \iint_{R_2} G\cos\theta\, du\, d\theta$$

$$= \int_{p_1}^{p_2}\int_{\theta_1}^{\pi/2} G\cos\theta\, du\, d\theta + \int_{p_2}^{\infty}\int_{\theta_1}^{\theta_2} G\cos\theta\, du\, d\theta$$

$$= \int_{p_1}^{p_2} G(1-\sin\theta_1)du + \int_{p_2}^{\infty} G(\sin\theta_2-\sin\theta_1)du \quad .$$

All the integrations have been performed above. The final result given below then represents the accelerated current under the condition of inequality given in (3.23)

$$I_{a_2} = \frac{J_a}{\sqrt{\pi}} e^{-\kappa^2}\left[\frac{a}{r_c}\sum_{n=o}^{\infty}\frac{\kappa^{2n}}{(n!)^2}\left\{\gamma\left(n+\frac{3}{2},\frac{p_2^2}{c^2}\right)-\gamma\left(n+\frac{3}{2},\frac{p_1^2}{c^2}\right)-\frac{\sigma r_c^2}{\tau^2 a}\left(\gamma\left(n+1,\frac{p_2^2}{c^2}\right)\right.\right.\right.$$

$$\left.\left.\left.-\gamma\left(n+1,\frac{p_1^2}{c^2}\right)\right)\right\}+e^{-V_o}\sum_{n=o}^{\infty}\frac{\kappa^n}{n!(-V_o)^{n/2}}\left\{\Gamma\left(n+\frac{3}{2},\frac{p_2^2}{c^2}-V_o\right)+\Gamma\left(n+\frac{3}{2},\frac{p_1^2}{c^2}-V_o\right)\right\} x$$

$$\left.J_n(2\kappa\sqrt{-V_o})\right] \quad . \qquad (3.24)$$

For $\kappa = 0$ it can be easily shown that Eq. (3.24) reduces to Eq. (3.22). The negative sign in front of the function $\gamma(n+3/2, p_1^2/c^2)$ in Eq. (3.24) is taken care of because the argument of the first error function in Eq. (3.22) is $-p_1/c$, as has been pointed out above, while the corresponding error function obtained by setting $\kappa = 0$ in Eq. (3.24) has the argument p_1/c. Since, however, $\mathrm{erf}(-p_1/c) = -\mathrm{erf}(p_1/c)$, the correct sign in front of the error function is automatically assured. Therefore, if $\kappa = 0$, Eq. (3.22) is the expression for

the accelerated current for both cases $p_1 > 0$ and $p_1 < 0$.

3.4 RETARDED CURRENT ($qV > 0$).

If the particles entering the sheath are repelled by the collector potential, Eqs. (3.9) or (3.13) define the domain for integrating (3.19) in association with the ranges of V given by the inequalities (3.12a) and (3.12b). Let us consider each case separately.

If $V_o \leq \sigma^2 r_c^2/\tau^2$, the domain of integration of (3.19) is represented by the dashed region enclosed between the two branches of the hyperbola shown in Fig. 3.2(b). However, this is the same domain as in the case of the current I_{a_2}. Thus the solution is of the same form as Eq. (3.24). Denoting by I_{r_1} the retarded current for the case $V_o \leq \sigma^2 r_c^2/\tau^2$, we have, therefore,

$$I_{r_1} = \frac{J_r}{\sqrt{\pi}} e^{-\kappa^2}\left[\frac{a}{r_c}\sum_{n=o}^{\infty}\frac{\kappa^{2n}}{(n!)^2}\left\{\gamma\left(n+\frac{3}{2},\frac{p_2^2}{c^2}\right)-\gamma\left(n+\frac{3}{2},\frac{p_1^2}{c^2}\right)-\frac{\sigma r_c}{\tau^2 a}\left(\gamma\left(n+1,\frac{p_2^2}{c^2}\right)\right.\right.\right.$$

$$\left.\left.\left.-\gamma\left(n+1,\frac{p_1^2}{c^2}\right)\right)\right\}+e^{-V_o}\sum_{n=o}^{\infty}\frac{\kappa^n}{n!\,V_o^{n/2}}\left\{\Gamma\left(n+\frac{3}{2},\frac{p_2^2}{c^2}-V_o\right)+\Gamma\left(n+\frac{3}{2},\frac{p_1^2}{c^2}-V_o\right)\right\}\times\right.$$

$$\left.I_n(2\kappa\sqrt{V_o})\right] \quad , \quad (3.25)$$

where $J_r = \sqrt{2\pi kT/m}\, Nq_r \ell r_c$ is the random current to the probe of the retarded particles of charge q_r and where the modified Bessel function $I_n(z)$ is defined by

$$I_n(z) = i^{-n} J_n(iz) \quad .$$

For $\kappa = 0$, Eq. (3.25) reduces to the following form:

$$I_{r_1}\Big|_{\kappa=0} = \frac{Jr}{2}\left[\frac{a}{r_c}\{\mathrm{erf}(\sqrt{\sigma^2 r_c^2-\tau^2 V_o}-\sigma a)+\mathrm{erf}(\sqrt{\sigma^2 r_c^2-\tau^2 V_o}+\sigma a)\}\right.$$

$$\left. + e^{-V_o}\{\mathrm{erfc}(\sqrt{\sigma^2 a^2-(1+\tau^2)V_o}-\sigma r_c)+\mathrm{erfc}(\sqrt{\sigma^2 a^2-(1+\tau^2)V_o}+\sigma r_c)\}\right] , \tag{3.26}$$

which is of the same form as Eq. (3,22) for the accelerated current.

It is evident from Eqs. (3.25) and (3.26) that in the presence of a magnetic field and $V_o \leq \sigma^2 r_c^2/\tau^2$ the current to the probe due to the retarded particles involves the parameter a/r_c which would not be the case in the absence of the magnetic field or when $V_o \geq \sigma^2 r_c^2/\tau^2$, as shown below.

If $V_o \geq \sigma^2 r_c^2/\tau^2$, the domain of integration of Eq. (3.19) is shown in Fig. 3.3. To integrate (3.19), we first need to find the minimum value of u. This may be done as follows:

The minimum value of u occurs when $\theta_1 = \theta_2$, i.e., where

$$\theta_1 = \sin^{-1}\left[\frac{\omega}{2u}\left(\frac{a^2-r_c^2}{a}\right) - \frac{r_c}{au}\sqrt{u^2 - \frac{2qV}{m}}\right]$$

$$= \sin^{-1}\left[\frac{\omega}{2u}\left(\frac{a^2-r_c^2}{a}\right) + \frac{r_c}{au}\sqrt{u^2 - \frac{2qV}{m}}\right] = \theta_2 \quad .$$

This gives $u_{min} = \sqrt{2qV/m}$. If I_{r_2} denotes the retarded current for the condition $V_o \geq \sigma^2 r_c^2/\tau^2$, then we write

$$I_{r_2} = \frac{2}{\sqrt{\pi}} \frac{a}{r_c} \frac{J_r}{c^3} e^{-\kappa^2} \int_{\sqrt{\frac{2qV}{m}}}^{\infty} du \int_{\theta_1}^{\theta_2} d\theta \; u \cos\theta \; e^{-u^2/c^2} I_o\left(2\kappa \frac{u}{c}\right)$$

$$= \frac{4}{\sqrt{\pi}} \frac{J_r}{c^3} e^{-\kappa^2} \int_{\sqrt{\frac{2qV}{m}}}^{\infty} u\sqrt{u^2 - \frac{2qV}{m}} \; e^{-u^2/c^2} I_o\left(2\kappa \frac{u}{c}\right) du \quad . \qquad (3.27)$$

Equation (3.27) is clearly independent of σ and a/r_c. From this we conclude that the retarded current to the probe is unaffected by the presence of the magnetic field whenever V_o is larger than or equal to $\sigma^2 r_c^2/\tau^2$. The integral in Eq. (3.27) has been evaluated by Kanal.[10] The result is

$$I_{r_2} = J_r \; e^{-V_o - \kappa^2} \sum_{n=o}^{\infty} \frac{(2n+1)!\,\kappa^n}{(n!)^2 2^{2n} V_o^{n/2}} I_n(2\kappa V_o^{1/2}) \quad . \qquad (3.28)$$

For values of $V_o = \sigma^2 r_c^2/\tau^2$, Eqs. (3.25) and (3.28) reduce to the following form:

$$I_r = J_r \exp\left(-\frac{\sigma^2 r_c^2}{\tau^2} - \kappa^2\right) \sum_{n=o}^{\infty} \frac{(2n+1)!}{(n!)^2 2^{2n}} \left(\frac{\kappa\tau}{\sigma r_c}\right)^n I_n\left(\frac{2\kappa\sigma r_c}{\tau}\right) \quad . \qquad (3.29)$$

For $\kappa = 0$, Eq. (3.29) becomes:

$$I_{r_2}\Big|_{\kappa=0} = J_r \exp\left(-\frac{\sigma^2 r_c^2}{\tau^2}\right) \quad . \qquad (3.30)$$

Equations (3.29) and (3.30) represent the current of the retarded particles at the point of transition, i.e., when $V_o = \sigma^2 r_c^2/\tau^2$.

3.5 DISCUSSION

All the equations we have derived are based on the assumption that the particles have a Maxwellian velocity distribution at the sheath edge and that the mean free path of the particles is sufficiently large to ensure a collisionless sheath. We have ignored the effect of the magnetic field on this distribution. Then in conjunction with a given sheath model (of Langmuir type) the current equations were derived for accelerating and retarding probe potentials. Thus for the accelerating potential we obtained Eq. (3.21), valid through the domain prescribed by the inequality (3.20), and Eq. (3.24) valid for the corresponding inequality given by (3.23). For $\kappa = 0$ both Eqs. (3.21) and (3.24) yield Eq. (3.22). For the retarding potential, Eq. (3.25) was obtained under the condition that $V_o \leq \sigma^2 r_c^2/\tau^2$. For $\kappa = 0$, this equation reduced to Eq. (3.26). For $V_o \geq \sigma^2 r_c^2/\tau^2$, we concluded that the magnetic field had no effect on the current as exhibited by Eq. (3.28). For $V_o = \sigma^2 r_c^2/\tau^2$ both Eqs. (3.25) and (3.28) reduced to Eq. (3.29) which, then, was specialized for $\kappa = 0$ to obtain Eq. (3.30).

In plotting the current characteristics one is usually faced with the problem of defining the sheath dimensions explicitly in relation to the probe potentials. In a plasma without a magnetic field one need consider the sheath dimensions only insofar as the accelerated current is concerned. This, however, is not the case when the magnetic field is present, since then, the retarded current for $V_o \leq \sigma^2 r_c^2/\tau^2$, also exhibits dependence on the sheath dimension as is clear from Eq. (3.25). Thus for a meaningful plot of the current characteristics it is imperative to seek a proper relation be-

tween V_o and a/r_c for both modes of current collection. The degree of accuracy of such a relation is of critical importance in avoiding the spurious behavior of the current characteristics in the acceleration region, as has been discussed in detail in the semiannual report.[3] One must obviously solve the sheath problem to obtain the above mentioned equation in order to be able to affix any physical meaning to the equations so far derived. On account of the absence of such a relation no volt-ampere characteristics can be included in this report.

IV. THEORY OF THE PLASMA WAVE PROBE

4.1 GENERAL EXPRESSION FOR THE AC RESPONSE

Work has been started on the derivation of the expression for the response of a probe to a plasma wave. The two cases of a low frequency wave and a high frequency wave will be treated separately. In this connection the low frequency range is defined as $\omega \ll t_r^{-1}$, where t_r is the time of reflection of an electron from the negative probe; and conversely the high frequency is the range where $\omega \gg t_r^{-1}$. So far the low frequency case has been solved. Work on the high frequency case will be carried out in the future.

If $\omega \ll t_r^{-1}$ then the phase of the wave remains essentially unchanged during the time the electron spends inside the sheath. Therefore, steady state conditions can be applied. We consider a Maxwellian electron distribution with a superposed longitudinal plasma wave,

$$f(\vec{r},\vec{v},t) = f_o(v) + f_1(\vec{r},\vec{v},t) \tag{4.1}$$

$$f_o(v) = \frac{N_o}{\pi^{3/2}} e^{-v^2} \tag{4.2}$$

where the velocity $\vec{v}$ is expressed in units of the thermal velocity c and

N_o = average electron number density

$c^2 = \frac{2KT}{m}$,

T = electron temperature

m = electron mass

K = Boltzmann's constant.

For a plasma described by the linearized Vlasov equation the perturbation f_1, proportional to $\exp[i(\vec{k}\cdot\vec{r}-\omega t)]$, is given by the expression[11]

$$f_1 = \frac{A}{k}\frac{v_k}{v_k-\eta}e^{-v^2} \quad , \tag{4.3}$$

where

v_k = component of $\vec{v}$ in the direction $\vec{k}$,

$\eta = \frac{\omega}{ck}$,

and $A(\vec{r},t)$ is assumed to be proportional to $\exp[i(\vec{k}\cdot\vec{r}-\omega t)]$.

The response of a cylindrical probe to a perturbation of the above form for the case where the probe makes an angle of 90° with the propagation vector $\vec{k}$ has been calculated. It is assumed that the diameter of the sheath surrounding the cylinder is small compared with the wavelength of the plasma wave. In that case all points on the sheath edge can be considered in phase so that the factor $e^{i\,\vec{k}\cdot\vec{r}}$ will be approximately uniform throughout the sheath. The parameter A is therefore taken to be of the form $Be^{-i\omega t}$, where B is constant inside the sheath.

In addition any diffraction of the wave by the probe is neglected; that is the wave is considered to be undisturbed by the probe.

The total current collected by the probe is then

$$I = acq \int_0^{\ell} dz \int_0^{2\pi} d\theta \int_{0,v_1}^{\infty} dv_r \int_{-v_{t_1}}^{v_{t_1}} dv_t \int_{-\infty}^{\infty} dv_z v_r f(z, r, \theta, v_r, v_t, v_z) \quad , \tag{4.4}$$

where

a = sheath radius,

ℓ = length of the cylinder,

q = charge of the particles under consideration,

z = coordinate axis along axis of cylinder,

θ = azimuth angle in the plane perpendicular to the axis of the cylinder,

v_r = radial velocity component in the plane perpendicular to the axis of the cylinder,

v_t = tangential velocity component in the plane perpendicular to the axis of the cylinder

v_z = velocity component along the z-axis.

The limits of the v_r and v_t integrations are determined from conservation of energy and angular momentum, namely

$$v_{t_1} = \tau\sqrt{v_r^2 - V_o} \quad , \qquad v_1^2 = V_o$$

where

$$\tau = \sqrt{\frac{r_c^2}{a^2 - r_c^2}} \quad ,$$

$$V_o = \frac{qV}{KT} \quad ,$$

V = potential of the collector with respect to the sheath edge,

r_c = radius of collector.

The collector potential is taken positive when the collector attracts the electrons. The lower limit of the v_r integration is 0 when $V_o < 0$ (accelerating potnetial) and v_1 when $V_o > 0$ (retarding potential). End effects due to the finite length of the cylinder are neglected.

Substitution of Eqs. (4.1), (4.2), and (4.3) into Eq. (4.4) gives an expression of the form

$$I = I_{DC} + I_{AC} \quad ,$$

where I_{DC} is the term involving the equilibrium distribution function f_o, and I_{AC} represents the response of the probe to the plasma wave f_1. In the development which follows we shall be concerned only with the AC component of the collector current. The DC component has been calculated previously by many authors. We have then

$$I_{AC} = Q \int_0^{2\pi} d\theta \int_{0,v_1}^{\infty} dv_r \int_{-v_{t_1}}^{v_{t_1}} dv_t \, \frac{v_r v_k}{v_k - \eta} \, e^{-(v_r^2 + v_t^2)} \quad ,$$

where Q is given by

$$Q = \frac{ac\ell Bq}{k} \, e^{-i\omega t} \int_{-\infty}^{\infty} e^{-v_z^2} \, dv_z$$

$$= \frac{ac\ell Bq\sqrt{\pi}}{k} \, e^{-i\omega t} \quad . \tag{4.5}$$

v_k can be expressed in terms of v_r and v_t, see Fig. 4.1, $v_k = v_r\cos\theta + v_t\sin\theta$.

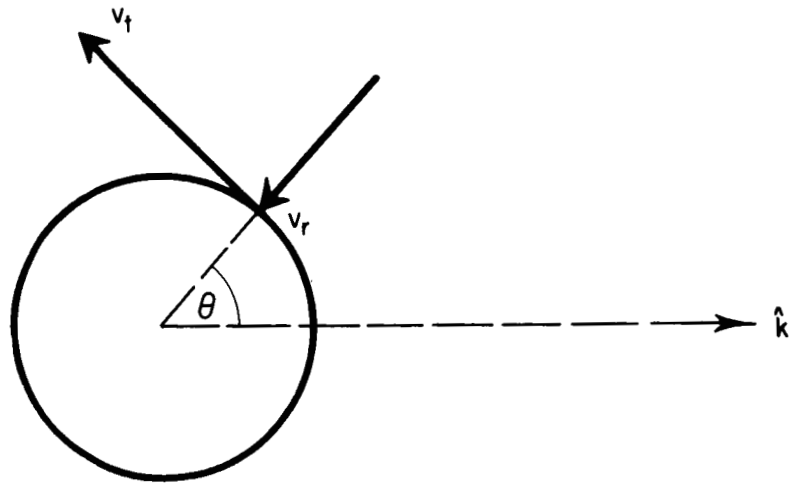

Fig. 4.1. Perpendicular cross section of the sheath edge showing relation of velocity components to wave vector $\vec{k}$.

Hence I_{AC} becomes

$$I_{AC} = Q\int_{o}^{2\pi} d\theta \int_{o,v_1}^{\infty} dv_r \int_{-v_{t_1}}^{v_{t_1}} dv_t v_r \frac{v_r\cos\theta+v_t\sin\theta}{v_r\cos\theta+v_t\sin\theta-\eta} e^{-(v_r^2+v_t^2)} .$$

The above integrand can be separated into two parts as follows

$$\frac{v_r\cos\theta+v_t\sin\theta}{v_r\cos\theta+v_t\sin\theta-\eta} = 1 + \frac{\eta}{v_r\cos\theta+v_t\sin\theta-\eta} .$$

Substituting those two terms into the expression for I_{AC} one obtains

$$I_{AC} = Q\left\{\int_{o}^{2\pi} d\theta \int_{o,v_1}^{\infty} dv_r \int_{-v_{t_1}}^{v_{t_1}} dv_t v_r\, e^{-(v_r^2+v_t^2)} + \eta\int_{o}^{2\pi} d\theta \int_{o,v_1}^{\infty} dv_r \int_{-v_{t_1}}^{v_{t_1}} dv_t \frac{v_r\, e^{-(v_r^2+v_t^2)}}{v_r\cos\theta+v_t\sin\theta-\eta}\right\} , \quad (4.6)$$

where Q is given by Eq. (4.5). Equation (4.6) is the general expression for

the AC response of a probe to a plasma wave under the assumptions stated above.

Integration of the first term is elementary. The result is

$$J_1 \equiv \int_0^{2\pi} d\theta \int_{0,v_1}^{\infty} dv_r \int_{-v_{t_1}}^{v_{t_1}} dv_t v_r \, e^{-(v_r^2+v_t^2)}$$

$$= \begin{cases} \pi^{3/2}\left[\operatorname{erf}(\tau\sqrt{-V_o}) + \frac{r_c}{a} e^{-V_o}\operatorname{erfc}(\sqrt{-V_o(1+\tau^2)})\right] & \text{if } V_o < 0 \\ \pi^{3/2} \frac{r_c}{a} e^{-V_o} & \text{if } V_o > 0 \end{cases} \qquad (4.7)$$

where

$$\operatorname{erf}(x) = \frac{2}{\sqrt{\pi}} \int_0^x e^{-y^2} dy$$

and

$$\operatorname{erfc}(x) = 1 - \operatorname{erf}(x) \quad .$$

4.2 ACCELERATING POTENTIAL

In carrying out the integration of the second term, the case of the accelerating potential ($V_o < 0$) will be considered first. After the following transformation of the variables of integration

$$v_r = u \cos\phi$$

$$v_t = u \sin\phi$$

$$dv_r dv_t = u \, du \, d\phi$$

the integral becomes

$$J_2^- = \int_0^{2\pi} d\theta \iint_{\Omega^-} \frac{u^2 \cos\phi \; e^{-u^2}}{u\cos(\theta-\phi)-\eta} \, du \, d\phi \quad . \tag{4.8}$$

Ω^- is the region bounded by the two hyperbolas $v_{t_1} = \pm\tau\sqrt{v_r^2 - V_o}$, as shown by the shaded area in Fig. 4.2.

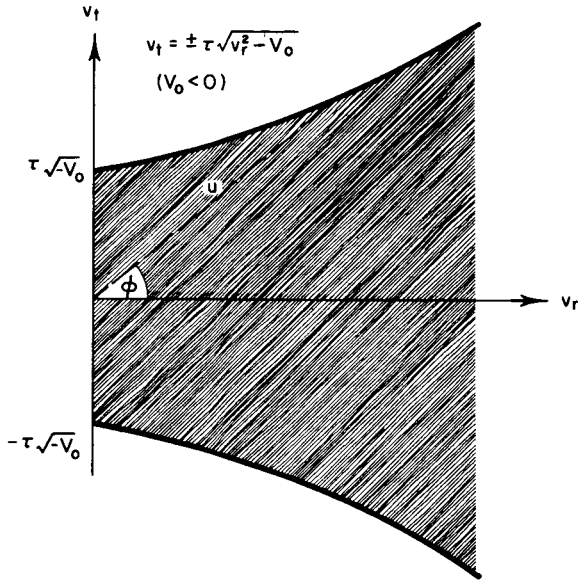

Fig. 4.2. Region of integration Ω^- for the case of an accelerating potential $(V_o < 0)$.

In terms of the variables u, ϕ the region of integration is given by the expressions

$$-\frac{\pi}{2} \le \phi \le \frac{\pi}{2} \quad \text{for} \quad 0 \le u \le \tau\sqrt{-V_o}$$

$$-\phi_1 \le \phi \le \phi_1 \quad \text{for} \quad \tau\sqrt{-V_o} \le u \le \infty \quad ,$$

where

$$\phi_1 = \sin^{-1}\left[\frac{\tau}{\sqrt{1+\tau^2}}\sqrt{\frac{u^2 - V_o}{u^2}}\right] \quad .$$

As shown in Appendix A the Θ-integration gives the following result

$$\frac{1}{u}\int_0^{2\pi} \frac{d\Theta}{\cos(\Theta-\phi) - \frac{\eta}{u}} = \begin{cases} 0 & u > \eta \\ -\frac{2\pi}{\sqrt{\eta^2-u^2}} & u < \eta \end{cases} \tag{4.9}$$

Hence, after substitution of Eq. (4.9) into Eq. (4.8) the following result is obtained,

$$\bar{J}_2 = \begin{cases} -2\pi \int_0^{\eta} du \int_{-\pi/2}^{\pi/2} d\phi \, \frac{u^2 e^{-u^2}\cos\phi}{\sqrt{\eta^2-u^2}} & \eta < \tau\sqrt{-V_o} \qquad (4.10a) \\ -2\pi \left\{ \int_0^{\tau\sqrt{-V_o}} du \int_{-\pi/2}^{\pi/2} d\phi \, \frac{u^2 e^{-u^2}\cos\phi}{\sqrt{\eta^2-u^2}} + \int_{\tau\sqrt{-V_o}}^{\eta} du \int_{-\phi_1}^{\phi_1} d\phi \, \frac{u^2 e^{-u^2}\cos\phi}{\sqrt{\eta^2-u^2}} \right\}, & \\ \eta > \tau\sqrt{-V_o} \qquad (4.10b) \end{cases}$$

where

$$\phi_1 = \sin^{-1}\left[\frac{\tau}{\sqrt{1+\tau^2}}\sqrt{\frac{u^2-V_o}{u^2}}\right] .$$

The regions of integration for the two above cases are shown in Figs. 4.3 and 4.4.

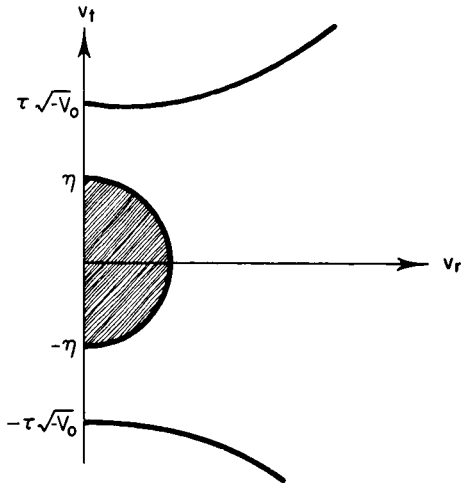

Fig. 4.3. Region of integration for an accelerating potential for the case $\eta < \tau\sqrt{-V_o}$.

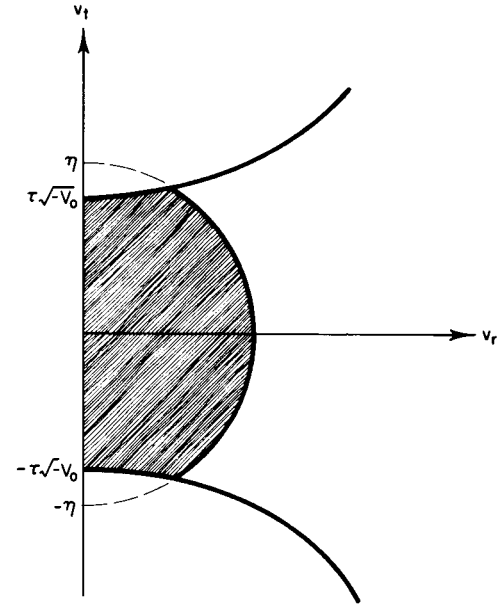

Fig. 4.4. Region of integration for an accelerating potential for the case $\eta > \tau\sqrt{-V_o}$.

The case $\eta < \tau\sqrt{-V_o}$ will be considered first. The ϕ-integration introduces a factor 2. Hence,

$$\bar{J}_{21} = -\frac{4\pi}{\eta}\int_o^{\eta} du\, \frac{u^2 e^{-u^2}}{\sqrt{1-\left(\frac{u}{\eta}\right)^2}} .$$

The above integral is evaluated in Appendix B. The result is, according to Eq. (B-2),

$$\bar{J}_{21} = \pi^2\eta^2 e^{-\eta^2/2}\left[I_1\left(\frac{\eta^2}{2}\right) - I_0\left(\frac{\eta^2}{2}\right)\right] \quad . \qquad \eta < \tau\sqrt{-V_o} \qquad (4.11)$$

This is the solution of the integral in Eq. (4.8) for the case where $\eta < \tau\sqrt{-V_o}$.

If $\eta > \tau\sqrt{-V_o}$, then $\bar{J}_2$ is a sum of two integrals [see Eq. (4.10b)]. After performing the integration with respect to ϕ this becomes

$$\bar{J}_{22} = -4\pi\left\{\int_o^{\tau\sqrt{-V_o}} du\, \frac{u^2 e^{-u^2}}{\sqrt{\eta^2-u^2}} + \frac{\tau}{\sqrt{1+\tau^2}}\int_{\tau\sqrt{-V_o}}^{\eta} du\, u\sqrt{\frac{u^2-V_o}{\eta^2-u^2}}\, e^{-u^2}\right\} \quad .$$

The solution of the first of these two integrals is obtained by setting $a = 0$, $b = \tau\sqrt{-V_o}$, and $c = 0$ in Eq. (B-1) of Appendix B while the solution of the second is obtained by setting $a = \tau\sqrt{-V_o}$, $b = \eta$, $c = -V_o$. Hence, $\bar{J}_{22}$ becomes

$$\bar{J}_{22} = -4\pi\left\{\frac{1}{2\eta}\sum_{m=o}^{\infty}\frac{\left(\frac{1}{2}\right)_m}{m!\,\eta^{2m}}\,\gamma\left(m+\frac{3}{2},\ -\tau^2V_o\right) + \frac{\tau}{\sqrt{1+\tau^2}}\,\frac{e^{-V_o}}{2\sqrt{\eta^2-V_o}}\sum_{m=o}^{\infty}\frac{\left(\frac{1}{2}\right)_m}{m!}\right.$$

$$\left.\frac{1}{(\eta^2-V_o)^m}\left[\gamma\left(m+\frac{3}{2},\ \eta^2-V_o\right) - \gamma\left(m+\frac{3}{2},\ -V_o(\tau^2+1)\right)\right]\right\} \quad . \qquad (4.12)$$

That part of the above sum containing the function $\gamma\left(m+\frac{3}{2},\ \eta^2-V_o\right)$ can be carried out by making use of Eq. (B-3), according to which

$$\frac{1}{2\sqrt{\eta^2-V_o}} \sum_{n=o}^{\infty} \frac{\left(\frac{1}{2}\right)^n}{n!} \frac{1}{(\eta^2-V_o)^n} \gamma\left(n+\frac{3}{2},\ \eta^2-V_o\right) =$$

$$= -\frac{(\eta^2-V_o)\pi}{4} e^{-(\eta^2-V_o)/2}\left[I_1\left(\frac{\eta^2-V_o}{2}\right) - I_o\left(\frac{\eta^2-V_o}{2}\right)\right] \quad . \qquad (4.13)$$

Eq. (4.12) may therefore be rewritten in the following way,

$$\bar{J}_{22} = -4\pi\left\{\frac{1}{2\eta} \sum_{m=o}^{\infty} \frac{\left(\frac{1}{2}\right)^m}{m!} \frac{1}{\eta^{2m}} \gamma\left(m+\frac{3}{2},\ -\tau^2 V_o\right) - \frac{\tau}{\sqrt{1+\tau^2}} \frac{e^{-V_o}}{2\sqrt{\eta^2-V_o}} \sum_{m=o}^{\infty} \frac{\left(\frac{1}{2}\right)^m}{m!}\right.$$

$$\left.\frac{1}{(\eta^2-V_o)^m} \gamma\left(m+\frac{3}{2},\ -V_o(\tau^2+1)\right)\right\} + \frac{\tau}{\sqrt{1+\tau^2}} \pi^2(\eta^2-V_o) e^{-(\eta^2+V_o)/2}\left[I_1\left(\frac{\eta^2-V_o}{2}\right)\right.$$

$$\left. - I_o\left(\frac{\eta^2-V_o}{2}\right)\right] \qquad \eta > \tau\sqrt{-V_o} \quad . \qquad (4.14)$$

Upon substitution of Eqs. (4.7), (4.11), and (4.14) into Eq. (4.6) the accelerated current finally becomes

$$\bar{I}_{AC} = \begin{cases} \frac{ac\ell Bq\sqrt{\pi}}{k} e^{-i\omega t}\left\{\pi^{3/2}\left[\operatorname{erf}(\tau\sqrt{-V_o}) + \frac{r_c}{a} e^{-V_o}\operatorname{erfc}(\sqrt{-V_o(1+\tau^2)})\right] + \eta\bar{J}_{21}\right\} & \eta < \tau\sqrt{-V_o} \\ \frac{ac\ell Bq\sqrt{\pi}}{k} e^{-i\omega t}\left\{\pi^{3/2}\left[\operatorname{erf}(\tau\sqrt{-V_o}) + \frac{r_c}{a} e^{-V_o}\operatorname{erfc}(\sqrt{-V_o(1+\tau^2)})\right] + \eta\bar{J}_{22}\right\} & \eta > \tau\sqrt{-V_o} \end{cases} \qquad (4.15)$$

where $\bar{J}_{21}$ and $\bar{J}_{22}$ are given by Eqs. (4.11) and (4.14) respectively.

4.3 RETARDING POTENTIAL

In the case of a retarding potential ($V_o > 0$) the lower limit of integration with respect to v_r in Eq. (4.6) is $v_1 = \sqrt{V_o}$. The first integral appearing in Eq. (4.6) has been solved for the case of $V_o > 0$. The solution

is given in Eq. (4.7). It is

$$J_1^+ = \int_0^{2\pi} d\theta \int_{\sqrt{V_o}}^{\infty} dv_r \int_{-v_{t_1}}^{v_{t_1}} dv_t v_r \, e^{-(v_r^2+v_t^2)} = \pi^{3/2} \frac{r_c}{a} e^{-V_o} \quad . \quad (4.16)$$

The second integral appearing in Eq. (4.6) is

$$J_2^+ = \int_0^{2\pi} d\theta \iint_{\Omega^+} du \, d\phi \, \frac{u^2 \cos\phi \, e^{-u^2}}{u\cos(\theta-\phi)-\eta} \quad , \quad (4.17)$$

where the variables of integration have again been transformed to polar coordinates and where the region of integration Ω^+ is given by the area bounded by the hyperbola $v_{t_1} = \pm\tau\sqrt{v_r^2-V_o}$, as shown in Fig. 4.5. The integration

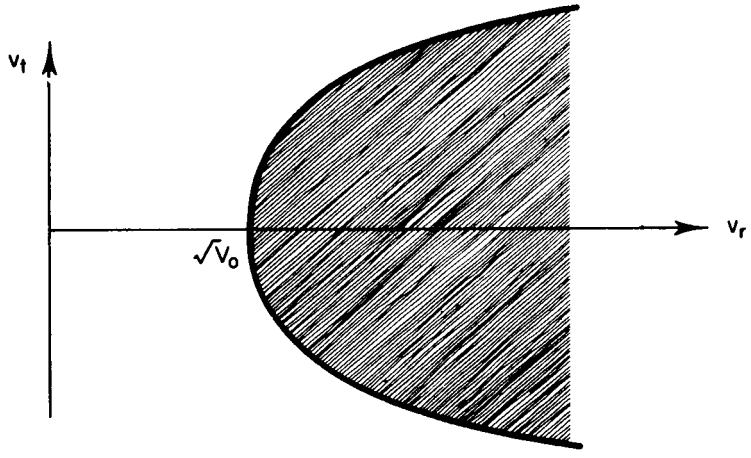

Fig. 4.5. Region of integration for retarding potential ($V_o > 0$).

with respect to θ has already been carried out in the section on the accelerating potential. The result is given by Eq. (4.9). In the integration over u and ϕ the two cases $\eta < \sqrt{V_o}$ and $\eta > \sqrt{V_o}$ have to be distinguished. The integral in Eq. (4.17) is non-vanishing only over the region of intersection of the circle of radius η with the area Ω^+, shown in Fig's. 4.6 and 4.7 for the two cases $\eta < \sqrt{V_o}$ and $\eta > \sqrt{V_o}$.

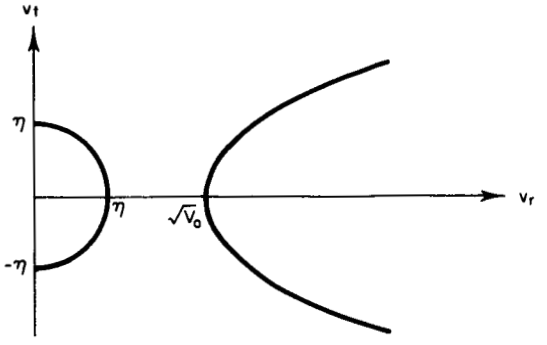

Fig. 4.6. Region of integration for the case $\eta < \sqrt{V_o}$.

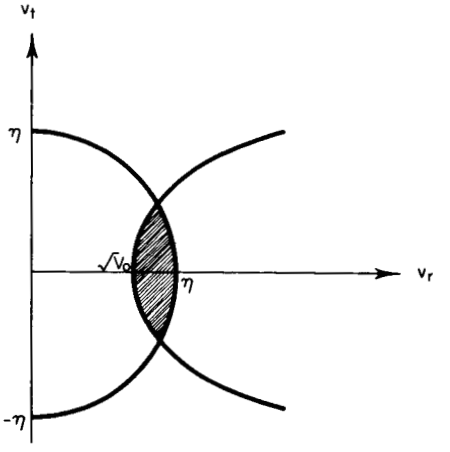

Fig. 4.7. Region of integration for the case $\eta > \sqrt{V_o}$.

The region of intersection is shown shaded. It is seen that J_2^+ vanishes when $\eta < \sqrt{V_o}$. The rest of the treatment will therefore be devoted to the case $\eta > \sqrt{V_o}$. In that case Eq. (4.17) can be written in the form

$$J_2^+ = -2\pi \int_{\sqrt{V_o}}^{\eta} du \int_{-\phi_1}^{\phi_1} d\phi \, \frac{u^2 e^{-u^2} \cos\phi}{\sqrt{\eta^2 - u^2}} \quad , \tag{4.18}$$

where as before

$$\phi_1 = \sin^{-1}\left[\frac{\tau}{\sqrt{1+\tau^2}} \sqrt{\frac{u^2 - V_o}{u^2}}\right] \quad .$$

After the ϕ-integration this becomes

$$J_2^+ = -4\pi \frac{\tau}{\sqrt{1+\tau^2}} \int_{\sqrt{V_o}}^{\eta} u \, e^{-u^2} \sqrt{\frac{u^2 - V_o}{\eta^2 - u^2}} \, du \quad .$$

The above integral has been evaluated in Appendix B. Putting $a = \sqrt{V_o}$, $b = \eta$, $c = -V_o$ in Eq. (B-1) we obtain

$$J_2^+ = -2\pi \frac{\tau\, e^{-V_o}}{\sqrt{1+\tau^2}\sqrt{\eta^2-V_o}} \sum_{n=o}^{\infty} \frac{\left(\frac{1}{2}\right)_n}{n!} \frac{1}{(\eta^2-V_o)^n} \gamma\left(n+\frac{3}{2}, \eta^2-V_o\right) .$$

According to Eq. (4.13) this is equal to

$$J_2^+ = \frac{\pi^2\tau}{\sqrt{1+\tau^2}} (\eta^2-V_o) e^{-\eta^2+V_o/2} \left[I_1\left(\frac{\eta^2-V_o}{2}\right) - I_o\left(\frac{\eta^2-V_o}{2}\right) \right] . \qquad (4.19)$$

Hence, the retarded current is given by the following expression

$$I_{AC}^+ = \begin{cases} \frac{r_c c \ell B q \pi^2}{k} e^{-V_o} e^{-i\omega t} & \eta < \sqrt{V_o} \\ \frac{ac\ell Bq}{k} e^{-i\omega t} \left[\pi^2 \frac{r_c}{a} e^{-V_o} + \eta\sqrt{\pi}\, J_2^+ \right] & \eta > \sqrt{V_o} \end{cases} \qquad (4.20)$$

where J_2^+ is given by Eq. (4.19).

4.4 DISCUSSION

Equations (4.15) and (4.20) are the expressions for the accelerated and retarded AC currents, respectively. Both of these currents are proportional to $e^{-i\omega t}$. We conclude therefore that the current collected by the probe consists of the usual DC component plus a superposed AC component which oscillates with the frequency of the plasma wave. A detailed analysis of the amplitude of the AC response as a function of probe potential must await further calculations, especially the summing of the expression J_{22}^- given by Eq. (4.14). This work is being carried out at the present time. In addition the important question of whether or not the amplitude of the response is large enough for detection will be investigated.

Of particular interest is the limiting value of the response as the ratio r_c/a goes to zero. This limit depends, of course, on the value of the

potential V_o. In ionospheric applications, however, the probe radius will in general be small as compared with the Debye length. If the probe is at its equilibrium potential (i.e., if it is not driven), the sheath thickness is of the order of the Debye length λ_D. Therefore, if $r_c/\lambda_D \ll 1$, it follows that $r_c/a \ll 1$. As the probe is driven more negative than its equilibrium potential, the sheath radius increases and hence r_c/a decreases further. Taking the limit as $r_c/a \to 0$ one obtains for the AC current the following expressions

$$\lim_{\frac{r_c}{a} \to 0} I^{-}_{AC} = \frac{c\ell Bq}{k} e^{-i\omega t}\left\{\pi^2 r_c\left[\sqrt{-V_o} + e^{-V_o}\operatorname{erfc}\left(\sqrt{-V_o}\right)\right]\right.$$

$$+ 4\pi^{3/2}\eta\left[r_c \frac{e^{-V_o}}{2(\eta^2-V_o)} \sum_{m=o}^{\infty} \frac{\left(\frac{1}{2}\right)_m}{m!} \frac{1}{(\eta^2-V_o)^m} \gamma\left(m+\frac{3}{2},\ -V_o\right)\right]$$

$$\left. - \eta\, r_c\, \pi^{5/2}(\eta^2-V_o)\, e^{-\eta^2+V_o)/2}\left[I_1\left(\frac{\eta^2-V_o}{2}\right) - I_o\left(\frac{\eta^2-V_o}{2}\right)\right]\right\}$$

$$\eta > \frac{r_c}{a}\sqrt{-V_o} \qquad (4.15')$$

$$\lim_{\frac{r_c}{a} \to 0} I^{+}_{AC} = \begin{cases} \dfrac{r_c c\ell Bq\pi^2}{k} e^{-V_o} e^{-i\omega t} & \eta < \sqrt{V_o} \\ \dfrac{r_c c\ell Bq}{k} e^{-i\omega t}\left\{\pi^2 e^{-V_o+\eta}\pi^{3/2}(\eta^2-V_o)\, e^{-\eta^2+V_o)/2}\right. & \\ \left.\left[I_1\left(\dfrac{\eta^2-V_o}{2}\right) - I_o\left(\dfrac{\eta^2-V_o}{2}\right)\right]\right\} . & \eta > \sqrt{V_o} \end{cases} \qquad (4.20')$$

The limit of the accelerated current for the case $\eta < r_c/a\sqrt{-V_o}$ has not been computed since the phase velocity of the plasma wave always exceeds the

electron thermal velocity (i.e., $\eta > 1$), while $(r_c/a)\sqrt{-V_o} \ll 1$ has been assumed in taking the above limit.

Another limiting value of interest is the one as $a/r_c \to 1$. This limit occurs, when the probe potential approaches the plasma potential, and gives rise to the following expressions,

$$\lim_{\frac{a}{r_c} \to 1} I_{AC}^{-} = \frac{ac\ell Bq\pi^2}{k} e^{-i\omega t}\left\{\left[1 + \sqrt{\pi}\,\eta^3\, e^{-\eta^2/2}\left[I_1\left(\frac{\eta^2}{2}\right) - I_o\left(\frac{\eta^2}{2}\right)\right]\right\}\right. \qquad \eta < \tau\sqrt{-V_o} \tag{4.15"}$$

$$\lim_{\frac{a}{r_c} \to 1} I_{AC}^{+} = \begin{cases} \dfrac{r_c c\ell Bq\pi^2}{k} e^{-V_o} e^{-i\omega t} & \eta < \sqrt{V_o} \\ \dfrac{c\ell Bq\pi^2}{k} e^{-i\omega t}\left\{r_c\, e^{-V_o + a\eta\sqrt{\pi}(\eta^2 - V_o)} e^{-\eta^2 + V_o/2}\right. & \\ \left.\left[I_1\left(\dfrac{\eta^2 - V_o}{2}\right) - I_o\left(\dfrac{\eta^2 - V_o}{2}\right)\right]\right\}. & \eta > \sqrt{V_o} \end{cases} \tag{4.20"}$$

By varying the probe potential the experimenter can control whether the probe operates in the region where $a/r_c \to \infty$ or $a/r_c \to 1$.

The investigation is continuing with a view toward obtaining a better understanding of the general behavior of the plasma wave probe in all frequency regions so that it can be used for meaningful ionospheric measurements.

V. DISCUSSION

The study of the electron distribution as described in Section II shows that, considering only solar electromagnetic radiation as energy input and binary collisions as electron energy loss mechanism, a high energy hump in the energy distribution results. Drummond et al.,[9] have studied the question of stability of certain isotropic velocity distributions assuming a hump in the energy distribution. This work has shown that if the ambient electron temperature is low enough, the presence of such a hump may give rise to growing plasma waves. Such an instability would modify both the ambient electron distribution (i.e., the temperature) and the high energy hump in such a way as to quench the instability.

The investigation of the stability conditions for spherical plasma waves has been continued and is near completion. The result of this work will be described in a future report.

The electron energy distribution calculated in Section II is also being used to study the importance of the contribution of electron impact excitation to the total 6300Ø Å red line emission in the atmosphere.[12] The existence of a hump in the energy distribution may also be important in obtaining theoretical estimates of space craft equilibrium potential. Calculations to establish the significance of this hump on the equilibrium potential are being carried out.

It has been pointed out at the end of Section III that in order to obtain a meaningful voltage-current relation it is necessary to have an equation

which relates the sheath dimension to the probe potential. Approximate relations of this type have been derived for the case of no magnetic field; however the use of such a relation causes spurious results as was shown in the semiannual report.[3] For this reason a study of the sheath problem in the presence of a magnetic field has been started. A brief account of two methods thus employed is as follows:

Taking the cylindrical collector as an example (although the analysis holds equally well for spherical geometry), the first method[13] relies on the fact that in the absence of collisions the total currents carried by each kind of particles across two coaxial cylinders of arbitrary radii are equal. This enables one to determine the velocity distribution of the particles inside the sheath in terms of that in the undisturbed zone. Then, on obtaining the region of permissible velocities inside the sheath by means of Eqs. (3.5) and (3.6), the equation for the density of the particles may be derived by integrating the distribution function over that region of phase space. This method has the advantage of mathematical simplicity.

The other method for obtaining the density distribution function[14] relies on the fact that in the absence of collisions the general solution of Boltzmann's equation can be obtained by the method of characteristics. The general solution is an arbitrary function of the energy and angular momentum, and the precise function is then exactly determined by the boundary conditions.

After the density distribution function is evaluated by means of one of these methods, Poisson's equation serves to yield the potential distribution

inside the sheath. Both of these methods have been profitably employed in the case of zero magnetic field.[13,14] Work is in progress at this time to incorporate the effect of the magnetic field on the sheath structure.

The work described in Section IV is just the first step in what is expected to be a detailed study of the interaction between a probe and longitudinal plasma waves. At the present time the equations derived in Section IV are being analyzed further. The next step planned in this study is the investigation of the response of a probe to waves whose period is comparable or small compared to the time an electron spends inside the sheath.

REFERENCES

1. Nagy, A. F., Fontheim, E. G., and Dow, W. G., "Space Charge Waves in the Ionosphere and their Effect on the Heating of the Atmosphere," Trans. Am. Geophys. Union 43, 439, 1962.

2. Fontheim, E. G., Establishment of Stability by Collective Interactions in a Plasma with Collisions, Scientific Report 04613, 06106-1-S, Univ. of Mich., Space Physics Research Laboratory (March 1964).

3. Fontheim, E. G., Hoegy, W. R., and Kanal, M., A Theoretical Study of the Effect of Collective Interactions on the Electron Temperature in the Ionopshere and of the Langmuir Probe Characteristics in the Presence of a Magnetic Field, Semiannual Report No. 1, 06106-2-P, Univ. of Mich., Space Physics Research Laboratory (May 1964).

4. Hanson, W. B., "Electron Temperatures in the Upper Atmosphere," Space Research III (ed. W. Priester) 282, North Holland Publishing Co., Amsterdam, 1963.

5. Dalgarno, A. M., McElroy, M. B., and Moffett, R. J., "Electron Temperatures in the Ionosphere," Planetary Space Sci., 11, 463 (1963).

6. Geisler, J. E., and Bowhill, S. A., "Ionospheric Temperatures at Sunspot Minimum," J. Atmospheric Terrest. Phys. (to be published).

7. Butler, S. T., and Buckingham, M. J., "Energy Loss of a Fast Ion in a Plasma," Phys. Rev. 126, 1 (1962).

8. Watanabe, K., and Hinteregger, H. E., "Photoionization Rates in the E and F Regions," J. Geophys. Res. 67, 999 (1962).

9. Drummond, J. E., Nelson, D. J., and Hirshfield, J. L., Collision-Induced Instability in a Plasma with an Isotropic Velocity-Space Distribution, Boeing Scientific Laboratories, Report D1-82-0273(1963).

10. Kanal, M., "Theory of Current Collection of Moving Cylindrical Probes," J. Appl. Phys. 35, 1697 (1964).

11. Jackson, J. D., "Longitudinal Plasma Oscillations," Plasma Physics (Journal of Nuclear Energy, Part C) 1, 171 (1960).

12. Walker, J.C.G., and Dalgarno, A., "The Red Line of Atomic Oxygen in the Day Airglow," J. Atmos. Sci. 21, 463 (1964).

13. Mott-Smith, H. M., and Langmuir, I., "The Theory of Collectors in Gaseous Discharges," Phys. Rev. 28, 727 (1926).

14. Bernstein, I. B., and Rabinowitz, I. N., "Theory of Electrostatic Probes in a Low-Density Plasma," Phys. Fluids 2, 112 (1959).

APPENDIX A

Consider the integral

$$\int_0^{2\pi} \frac{d\theta}{\cos(\theta-\phi)-q} = \int_0^{2\pi} \frac{d\alpha}{\cos\alpha-q} \quad .$$

(a) $q < 1$.

In that case the integrand has a pole, and the integral has meaning only in the principal value sense. It is sufficient to evaluate the integral between the limits 0 and π. Then

$$\lim_{\epsilon\to 0} \int_0^{\alpha_0-\epsilon} \frac{d\alpha}{\cos\alpha-q} + \int_{\alpha_0+\epsilon}^{\pi} \frac{d\alpha}{\cos\alpha-q} \quad ,$$

where $\alpha_0 = \cos^{-1} q$

$$= \lim_{\epsilon\to 0} \frac{1}{\sqrt{1-q^2}} \log \frac{\sqrt{1-q^2}\,\tan\frac{\alpha_0-\epsilon}{2} - q + 1}{\sqrt{1-q^2}\,\tan\frac{\alpha_0-\epsilon}{2} + q - 1} - \frac{1}{\sqrt{1-q^2}} \log \frac{1-q}{q-1}$$

$$+ \frac{1}{\sqrt{1-q^2}} \log \frac{1-q}{q-1} - \frac{1}{\sqrt{1-q^2}} \log \frac{\sqrt{1-q^2}\,\tan\frac{\alpha_0+\epsilon}{2} - q + 1}{\sqrt{1-q^2}\,\tan\frac{\alpha_0+\epsilon}{2} + q - 1}$$

$$= 0 \quad .$$

(b) $q > 1$.

Let $z = e^{i\alpha}$; then $d\alpha = dz/iz$. The integral is then

$$\frac{2}{i}\oint_C \frac{dz}{z^2-2qz+1} \quad ,$$

where C is the unit circle. The roots of the denominater are at

$$z_1 = q - \sqrt{q^2-1} \quad \text{and} \quad z_2 = q + \sqrt{q^2-1} \quad .$$

Since $q > 1$, the two roots are real and z_1 lies inside the unit circle. Hence, using Cauchy's theorem we obtain

$$\frac{2}{i}\oint_C \frac{dz}{z^2-2qz+1} = -\frac{2\pi}{\sqrt{q^2-1}} \quad .$$

APPENDIX B

We consider an integral of the following form:

$$H_1 = \int_a^b du\, u \sqrt{\frac{u^2+c}{\eta^2-u^2}}\, e^{-u^2} \qquad a < b \quad , \qquad b \leq \eta$$

Putting $u^2 = x-c$, $u\,du = 1/2\,dx$, one obtains

$$H_1 = \frac{e^c}{2} \int_{a^2+c}^{b^2+c} dx \sqrt{\frac{x}{\eta^2-x+c}}\, e^{-x}$$

$$= \frac{1}{2} \frac{e^c}{\sqrt{\eta^2+c}} \int_{a^2+c}^{b^2+c} \sqrt{\frac{x}{1-\frac{x}{\eta^2+c}}}\, e^{-x} dx$$

$$= \frac{1}{2} \frac{e^c}{\sqrt{\eta^2+c}} \sum_{n=o}^{\infty} \frac{\left(\frac{1}{2}\right)_n}{n!} \frac{1}{(\eta^2+c)^n} \int_{a^2+c}^{b^2+c} x^{n+1/2} e^{-x} dx \quad ,$$

where the factorial function $(\alpha)_n$ is defined by $(\alpha)_n = \prod_{k=1}^{n} (\alpha+k-1)$,

$$= \frac{1}{2} \frac{e^c}{\sqrt{\eta^2+c}} \sum_{n=o}^{\infty} \frac{\left(\frac{1}{2}\right)_n}{n!} \frac{1}{(\eta^2+c)^n} \left[\gamma\left(n+\frac{3}{2},\, b^2+c\right) - \gamma\left(n+\frac{3}{2},\, a^2+c\right)\right] \quad , \quad \text{(B-1)}$$

where $\gamma(\alpha,x)$ is the incomplete gamma function defined by $\gamma(\alpha,x) = \int_o^x t^{\alpha-1} e^{-t} dt$.

Of special interest is the case $a = c = o$, $b = \eta$,

$$H_2 = \frac{1}{\eta} \int_0^{\eta} du \, \frac{u^2 e^{-u^2}}{\sqrt{1 - \frac{u^2}{\eta^2}}} \quad .$$

Let $u^2 = s\eta^2$, $u\,du = (\eta^2/2)\,ds$. Then

$$H_2 = \frac{\eta^2}{2} \int_0^{1} ds \, \frac{s^{1/2}}{\sqrt{1-s}} \, e^{-s\eta^2} \quad .$$

Let $s = \cos^2\theta$, $ds = -2 \sin\theta \cos\theta \, d\theta$. Then

$$H_2 = \eta^2 \int_0^{\pi/2} d\theta \, \cos^2\theta \, e^{-\eta^2 \cos^2\theta}$$

$$= \frac{\eta^2}{2} \left\{ e^{-\eta^2/2} \int_0^{\pi/2} d\theta \, e^{(\eta^2/2)\cos 2\theta} + e^{-\eta^2/2} \int_0^{\pi/2} d\theta \, \cos 2\theta \, e^{(\eta^2/2)\cos 2\theta} \right\} .$$

Let $2\theta = \alpha$, $d\theta = 1/2 \, d\alpha$. Then

$$H_2 = \frac{\eta^2}{4} e^{-\eta^2/2} \left\{ \int_0^{\pi} d\alpha \, e^{(\eta^2/2)\cos\alpha} + \int_0^{\pi} d\alpha \, \cos\alpha \, e^{(\eta^2/2)\cos\alpha} \right\}$$

$$= \frac{\eta^2}{4} e^{-\eta^2/2} \left\{ \pi I_0\left(\frac{\eta^2}{2}\right) - \pi I_1\left(\frac{\eta^2}{2}\right) \right\} \quad , \qquad \text{(B-2)}$$

where $I_n(z)$ is the modified Bessel function of the first kind of index n defined by $I_n(z) = i^{-n} J_n(iz)$ and $J_n(z)$ is the Bessel function of the first kind of index n.

This result can be used to sum an infinite series of incomplete Gamma functions. Setting $a = c = o$, $b = \eta$ in Eq. (B-1), equating with H_2, and

using Eq. (B-2) one obtains

$$\frac{1}{2\eta}\sum_{n=o}^{\infty}\frac{\left(\frac{1}{2}\right)_n}{n!}\frac{1}{\eta^{2n}}\gamma\left(n+\frac{3}{2},\ \eta^2\right) = \frac{\eta^2}{4}e^{-\eta^2/2}\left[\pi I_o\left(\frac{\eta^2}{2}\right)-\pi I_1\left(\frac{\eta^2}{2}\right)\right] \quad . \qquad (B\text{-}3)$$